12-16-2004

Gas-phase chemical characteristics of Asian emission plumes observed during ITCT 2K2 over the eastern North Pacific Ocean

J. B. Nowak
National Oceanic and Atmospheric Administration

D. D. Parrish
National Oceanic and Atmospheric Administration

J. A. Neuman
National Oceanic and Atmospheric Administration

J. S. Holloway
National Oceanic and Atmospheric Administration

O. R. Cooper
National Oceanic and Atmospheric Administration

See next page for additional authors

Recommended Citation

Nowak, J. B., et al. (2004), Gas-phase chemical characteristics of Asian emission plumes observed during ITCT 2K2 over the eastern North Pacific Ocean, J. Geophys. Res., 109, D23S19, doi:10.1029/2003JD004488.

Gas-phase chemical characteristics of Asian emission plumes observed during ITCT 2K2 over the eastern North Pacific Ocean

J. B. Nowak,[1,2] D. D. Parrish,[1] J. A. Neuman,[1,2] J. S. Holloway,[1,2] O. R. Cooper,[1,2] T. B. Ryerson,[1] D. K. Nicks Jr.,[1,2,3] F. Flocke,[4] J. M. Roberts,[1] E. Atlas,[4,5] J. A. de Gouw,[1,2] S. Donnelly,[4,6] E. Dunlea,[1,2] G. Hübler,[1,2] L. G. Huey,[7] S. Schauffler,[4] D. J. Tanner,[7] C. Warneke,[1,2] and F. C. Fehsenfeld[1,2]

Received 23 December 2003; revised 26 March 2004; accepted 5 April 2004; published 21 July 2004.

[1] The gas-phase chemical characteristics of emission plumes transported from Asia across the Pacific Ocean observed during the Intercontinental Transport and Chemical Transformation experiment in 2002 (ITCT 2K2) are described. Plumes measured in the troposphere from an aircraft were separated from the background air in data analysis using 1-s measurements of carbon monoxide (CO), total reactive nitrogen (NOy), and other gas-phase species along with back trajectory analysis. On the basis of these measurements, Asian transport plumes with CO mixing ratios greater than 150 ppbv were observed on seven flights. Correlations between 1-s observations of CO, ozone (O_3), and NOy are used to characterize the plumes. The NOy/CO ratios were similar in each plume and significantly lower than those derived from estimated Asian emission ratios, indicating substantial removal of soluble NOy species during transport. Observations of nitric oxide (NO), nitrogen dioxide (NO_2), nitric acid (HNO_3), peroxyacetyl nitrate (PAN), peroxypropionyl nitrate (PPN), and alkyl nitrates are used with the NOy measurements to further distinguish the transport plumes by their NOy partitioning. NOy was primarily in the form of PAN in plumes that were transported in cold high-latitude and high-altitude regions, whereas in plumes transported in warmer, lower latitude and altitude regions, NOy was mainly HNO_3. Additional gas-phase species enhanced in these plumes include sulfuric acid, methanol, acetone, propane, and ethane. The O_3/CO ratio varied among the plumes and was affected by the mixing of anthropogenic and stratospheric influences. The complexity of this mixing prevents the determination of the relative contribution of anthropogenic and stratospheric influences to the observed O_3 levels. *INDEX TERMS:* 0345 Atmospheric Composition and Structure: Pollution—urban and regional (0305); 0365 Atmospheric Composition and Structure: Troposphere—composition and chemistry; 0368 Atmospheric Composition and Structure: Troposphere—constituent transport and chemistry; *KEYWORDS:* intercontinental transport, reactive nitrogen, emission plumes, ITCT 2K2

Citation: Nowak, J. B., et al. (2004), Gas-phase chemical characteristics of Asian emission plumes observed during ITCT 2K2 over the eastern North Pacific Ocean, *J. Geophys. Res.*, *109*, D23S19, doi:10.1029/2003JD004488.

1. Introduction

[2] Economic and industrial growth in Asia over the last few decades has resulted in increased emissions, both gas-phase and particulate, from industrial, transportation, power generation, and biomass burning sources into the atmosphere [*Kato and Akimoto*, 1992; *van Aardenne et al.*, 1999; *Streets and Waldhoff*, 2000; *Carmichael et al.*, 2002]. Previous work, both observational and theoretical, has studied the outflow of these emissions to the troposphere over western and central North Pacific [*Hoell et al.*, 1996, 1997; *Huebert et al.*, 2003; *Jacob et al.*, 2003; and references therein]. Observation-based studies have reported the transport of these emissions to the eastern Pacific and western United States [*Parrish et al.*, 1992; *Jaffe et al.*, 1999, 2001, 2003a, 2003b; *Kotchenruther et al.*, 2001a; *Moore et al.*, 2003; *Price et al.*, 2003]. Additional studies suggest that emissions from Asia can affect tropospheric

[1]Aeronomy Laboratory, National Oceanic and Atmospheric Administration, Boulder, Colorado, USA.
[2]Cooperative Institute for Research in Environmental Sciences, University of Colorado, Boulder, Colorado, USA.
[3]Now at Ball Aerospace and Technologies Corporation, Boulder, Colorado, USA.
[4]Atmospheric Chemistry Division, National Center for Atmospheric Research, Boulder, Colorado, USA.
[5]Now at Division of Marine and Atmospheric Chemistry, Rosenstiel School of Marine and Atmospheric Sciences, University of Miami, Miami, Florida, USA.
[6]Now at Department of Chemistry, Fort Hays State University, Hays, Kansas, USA.
[7]School of Earth and Atmospheric Sciences, Georgia Institute of Technology, Atlanta, Georgia, USA.

0148-0227/04/2003JD004488

trace gas concentrations and photochemistry in the western United States. For example, modeling studies indicate that the long-range transport of Asian emissions may contribute to an increase in background surface ozone (O_3) mixing ratios in the United States of 4–7 ppbv [*Fiore et al.*, 2002]. Therefore understanding the influence of long-range transport on tropospheric trace gas background levels may be crucial to determining the success of efforts to improve regional air quality.

[3] The Intercontinental Transport and Chemical Transformation experiment in 2002 (ITCT 2K2) was designed to study the long-range transport of trace gases and aerosols and their effect on background tropospheric levels of these species. ITCT 2K2 was conducted during April and May of 2002 from the west coast of the United States with ground-based measurements made at Trinidad Head, California, and airborne measurements from the National Oceanic and Atmospheric Administration (NOAA) WP-3D based in Monterey, California. Also included in the ITCT 2K2 effort was extensive meteorological analysis and numerical modeling of long-range transport to forecast the transport of Asian emission plumes across the Pacific Ocean.

[4] Here we report observations of various gas-phase species made in the free troposphere in air masses not directly influenced by North American sources. These observations are used to distinguish transported plumes of Asian emissions from the background tropospheric air. Relationships between important trace gases from these observations are also examined. The gas-phase chemical characteristics of three Asian emission plumes are discussed in detail. Several recent works examine additional aspects of these plumes. *Brock et al.* [2004] describe the chemical and microphysical characteristics of aerosols observed during ITCT 2K2 and in two of the three emission plumes described here. The source signatures observed in these Asian emission plumes are discussed by *de Gouw et al.* [2004]. *Cooper et al.* [2004a, 2004b] provide detailed meteorological analysis of two transport plumes described here.

2. Instrumentation and Methodology

2.1. Aircraft Measurements, Back Trajectories, and Sampling Strategy

[5] Eleven flights lasting up to 8 hours covering altitudes from 0 to 8 km were made by the NOAA WP-3D (http://www.aoc.noaa.gov) out of Monterey, California, during ITCT 2K2. Two transit flights were also made: (1) Tampa, Florida, to El Paso, Texas, to Monterey, California, and (2) Monterey, Calfornia, to Broomfield, Colorado. Though a primary goal was the characterization of Asian emission plumes, sorties were also flown to study the emissions from coastal shipping, forest fires, and urban areas, such as Los Angeles and San Francisco, California [*de Gouw et al.*, 2003b; *Neuman et al.*, 2003; G. Chen et al., manuscript in preparation, 2004]. The WP-3D was fitted with instruments to characterize both the gas-phase and aerosol characteristics of the Asian transport plumes. The 1-s time response for many of these instruments allowed for high-spatial-resolution measurements both vertically and horizontally. Details concerning the aerosol instrumentation are given by *Brock et al.* [2004]. Meteorological and navigational measurements were provided by the NOAA Aircraft Operations Center (http://www.aoc.noaa.gov). The gas-phase instrumentation used aboard the WP-3D has been previously discussed in detail elsewhere so only brief descriptions are given here.

[6] Carbon monoxide (CO) was measured using a vacuum-UV fluorescence technique described by *Holloway et al.* [2000]. During ITCT 2K2 this instrument measured CO at 1 Hz with a detection limit <1 ppbv, a precision of ±(1 ppbv + 2.5%), and an accuracy of 2% traceable to a NIST reference standard.

[7] Ozone (O_3) was measured by a chemiluminescence technique based upon the reaction of ambient O_3 and nitric oxide (NO) added as a reagent gas [*Ridley et al.*, 1992] and calibrated using an UV absorption instrument. Details concerning this version of the instrument can be found in the work of *Ryerson et al.* [1998]. During ITCT 2K2, O_3 was measured at 1 Hz with a 1σ precision of ±0.2 ppbv and ±2% accuracy.

[8] Total reactive nitrogen (NOy), nitrogen dioxide (NO_2), and NO were each measured using ozone-induced chemiluminescence. NO_2 was measured using the difference between the NO measurement and a separate measurement of NO preceded by a UV-photolysis cell [*Ryerson et al.*, 2000]. NO_y was measured using catalytic reduction on a 300°C gold converter followed by NO chemiluminescence detection [*Ryerson et al.*, 1999]. The conversion efficiency of the NOy instrument for nitrate aerosol is uncharacterized. However, the inlet design and orientation (sampling air perpendicular to the direction of flight) probably discriminates against the majority of aerosol by mass [*Ryerson et al.*, 1999]. During ITCT 2K2 each was measured at 1 Hz with the following uncertainties: NO, ±(15 pptv + 5%); NO_2, ±(30 pptv + 10%); and NO_y, ±(15 pptv + 10%).

[9] Nitric acid (HNO_3) was measured at 1 Hz with a chemical ionization mass spectrometry (CIMS) instrument described by *Neuman et al.* [2002]. During ITCT 2K2 the instrument sensitivity, as determined by in-flight calibrations, varied between 0.5 Hz/pptv (at high altitude) and 1.0 Hz/pptv (at lower altitudes). The accuracy of the calibration source was estimated at ±15%. Overall accuracy was estimated at ±(30 pptv + 15%) which reflects additional uncertainties caused by changes in the measured instrument background. The 1σ precision for the 1-Hz data was ±25 pptv.

[10] Peroxyacetyl nitrate (PAN) and peroxypropionyl nitrate (PPN) were measured every 1 to 2 min by a dual channel capillary gas chromatograph with electron capture detection (GC/ECD) as described by F. A. Flocke et al. (manuscript in preparation, 2004). The overall uncertainty for PAN and PPN was estimated to be less than ±(5 pptv + 15%).

[11] A number of volatile organic compounds (VOCs) were measured using proton transfer reaction mass spectrometry (PTR-MS) as described by *de Gouw et al.* [2003a]. During ITCT 2K2 data were reported every 10–15 s. Only the acetonitrile, methanol, acetone, benzene, and toluene data are used here because they have the most complete coverage in Asian transport plumes. The detection limit, determined mostly by counting statistics, for each was estimated at ±50 pptv. The calibration accuracy for the data

presented here was estimated to be ±15%. In PTR-MS, only the mass of protonated VOCs is determined and possibility of interference by other VOCs needs to be considered. Recent work has shown that interference was only a minor problem for the species discussed here [*Warneke et al.*, 2003; *de Gouw et al.*, 2003c].

[12] Up to 80 whole-air samples (WAS) were collected in stainless steel canisters during each flight. The collection time was approximately 8–12 s depending on altitude. The samples were analyzed offline by various chromatographic techniques [*Heidt et al.*, 1989; *Schauffler et al.*, 1999]. Analyzed species included alkyl nitrates, alkanes, alkenes, alkynes, chloroflourocarbons, and several aromatic compounds. Only the sum of the measured alkyl nitrates (methyl-, 2-butyl-, pentyl, 2-pentyl-, 3-pentyl-, ethyl-, 1-propyl-, and 2-propyl nitrate), propane, and ethane are used in this study. The estimated uncertainty in the alkyl nitrate measurements was ±20% [*Atlas et al.*, 1992].

[13] One-hertz carbon dioxide (CO_2) measurements were made using a modified Licor nondispersive infrared absorption instrument, which was calibrated in-flight to reference gases tied to NOAA Climate Monitoring and Diagnostics Laboratory (CMDL) standards; CO_2 measurement precision was estimated as ±0.08 ppmv and accuracy as ±0.2 ppmv [*Nicks et al.*, 2003].

[14] Sulfur dioxide (SO_2) measurements were made using a TECO 43C-TL pulsed fluorescence instrument that has been modified for aircraft operation [*Ryerson et al.*, 1998]. The estimated precision of the data was ±(0.35 ppbv + 6%). The uncertainty of the calibration standard was estimated ±2%.

[15] Sulfuric acid (H_2SO_4) was measured by chemical ionization/mass spectrometry (CIMS) [*Eisele and Tanner*, 1993] for a 1.1-s period every 4 s with an accuracy of ±35%, a precision of 1×10^6 molecules cm^{-3}, and a 3σ detection limit of $\sim 6 \times 10^6$ molecules cm^{-3}.

[16] Back trajectories were calculated with the FABtraj model, which uses the 1° × 1° NCEP FNL wind fields. An 8-day back trajectory was calculated for every minute of each flight from the aircraft position with the following output parameters: latitude, longitude, altitude, pressure, temperature, relative humidity, and potential vorticity. More details are given by *Cooper et al.* [2004a, 2004b].

2.2. Definition of Asian Transport Plumes

[17] Long-range transport of Asian emissions is viewed here in two ways: as episodic events and as that resulting from continual mixing of emissions into the background atmosphere. Episodic events are concentrated plumes that are clear enhancements above the background. The latter refers to the constant mixing of emission plumes into the background atmosphere that significantly influence the background concentrations over longer timescales. Several studies examining both episodic and diluted long-range transport are reported in the literature [*Bernsten et al.*, 1999; *Jacob et al.*, 1999; *Jaffe et al.*, 2003a, 2003b]. When examining long-range transport as episodic events, it is necessary to parse the emission plumes from the regional background atmosphere and from air masses that have been influenced by local and regional North American sources.

[18] In this study the primary gas-phase tracer used to identify Asian transport is CO because it is emitted from many anthropogenic sources and has a tropospheric lifetime similar to that of intrahemispheric mixing (1–3 months). All ITCT 2K2 CO data were divided into marine free troposphere (FT) and nonmarine categories. The marine FT data are taken above the marine boundary layer (MBL) estimated with available positional, meteorological, chemical, and aerosol data. MBL data were excluded to minimize the influence of local anthropogenic sources such as coastal shipping. Select data taken over the North American coast are included in the marine FT category provided the data were taken at altitudes greater than 1 km above the continental planetary boundary layer (PBL) within 250 km of the coast, the wind was from a predominantly westerly direction, and the data show no recent anthropogenic influence. This filter excluded much of the data from the two transit flights, 22 April and 19 May, and the urban air studies over San Francisco, 8 May, and Los Angeles, 13 May. The data were further filtered to remove any recent anthropogenic sources, such as aircraft plumes at altitude characterized by brief durations of high concentrations of NOy, NOx, and/or particles. Furthermore, the 8-day back trajectories were used to verify that none of the marine FT data had recently passed over the North American continent at low altitudes.

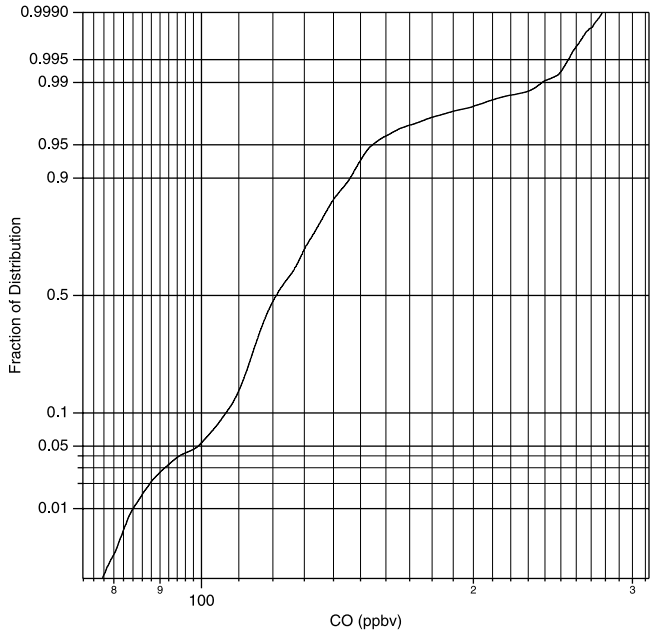

Figure 1. Cumulative probability graph of all ITCT 2K2 marine FT CO data.

[19] The resulting marine FT CO data are plotted on a cumulative probability graph in Figure 1. CO is lognormally distributed from approximately 100 to 150 ppbv, accounting for 90% of the marine FT CO observations. Two additional CO distributions are seen above 150 ppbv, from approximately 153 to 250 ppbv and greater than 250 ppbv. Combined, these two elevated distributions account for only 7% of all marine FT CO observations. On the basis of the cumulative distribution graph, Asian transport plumes are identified by CO mixing ratios above 150 ppbv.

[20] Previous studies have defined transport episodes or enhancements as deviations above the mean background

[*Talbot et al.*, 1997] or by statistical testing to determine significant differences between Asian and non-Asian back trajectory categories [*Jaffe et al.*, 1999]. A difficulty with the first method is the uncertainty in determining the mean background level of a tracer species, such as CO, because the mean of the data set is itself influenced by the transport events. *Jaffe et al.* [1999] identify two difficulties with using back trajectories as the primary method to separate out the transport. First, though an Asian back trajectory is calculated, a statistically significant enhancement is not always seen in the transport tracers. Second, enhancements have been seen in air masses in which the available 7–10 day back trajectories do not go back to Asia. However, these air masses show evidence of influence from anthropogenic sources in Asia even though the back trajectories are not conclusive. Additionally, trajectory analysis typically becomes more uncertain the farther back in time of the analysis. The methodology used here identifies the transported Asian emission plumes without prior knowledge of mean background levels and with supporting evidence from the back trajectory ensembles.

[21] Figure 1 shows a shift in the observed distribution of marine FT CO at high mixing ratios, such that 150 ppbv is a conservative lower limit to identify transport episodes. While CO mixing ratios above 150 ppbv are clearly linked with Asian sources, interpretation of the majority of observed marine FT CO data, 100 to 150 ppbv, is more difficult. *Novelli et al.* [1998] show that anthropogenic and biomass burning emissions over the last few decades have affected the background CO concentration throughout the Northern Hemisphere, even at remote sites. The lognormal distribution from 100 to 150 ppbv likely results from the mixing of natural, anthropogenic, and biomass burning CO emissions varying in source strength over different time and geographic scales. The extent to which the marine FT CO background distribution observed during ITCT 2K2 has been affected by the long-range transport of Asian emissions is not determined in the analysis presented here. Although emission plumes of varying CO concentrations are exported from Asia into the atmosphere over the Pacific, for the ITCT 2K2 data set, only those greater than 150 ppbv are unambiguously identified as distinct from the background.

[22] In summary, the Asian transport plumes encountered during ITCT 2K2 are defined for this analysis as those where (1) the air mass is marine FT at the time of sampling; (2) CO levels were greater than 150 ppbv; and (3) the associated back trajectories indicate that the air mass passed over or originated in Asia and had not encountered anthropogenic influences from North America before sampling. All marine FT data were subdivided into two categories on the basis of the use of CO as an Asian transport tracer: transport plumes (as defined above) and background, which is the subset of data remaining after the transport data have been removed from the marine FT category.

3. Observations and Analysis

3.1. Transport Plumes

[23] A summary of the average and standard deviations of gas-phase data collected during ITCT 2K2 for each category is given in Table 1. Even though the flight planning was designed to sample Asian transport plumes, only 7% of all marine FT CO data was 150 ppbv or greater. Of all the species listed in Table 1, a 2σ or greater enhancement compared to the average marine FT background value was observed within transport plumes only for CO, NOy, PAN, PPN, H_2SO_4, acetone, ethane, and propane. However, as will be seen when examining the individual transport flights, grouping all transport plume data observed during ITCT masks much of the variability seen in the individual plumes.

Table 1. Marine FT, Marine FT Background, and Transport Plume Statistics[a]

Species	Marine FT	Marine Background FT	Transport Plumes
CO	125 ± 23	122 ± 14	198 ± 40
O_3	59 ± 14	59 ± 14	73 ± 10
NO_y	0.32 ± 0.17	0.30 ± 0.16	0.64 ± 0.16
HNO_3	0.05 ± 0.09	0.05 ± 0.1	0.07 ± 0.1
PAN	0.16 ± 0.1	0.15 ± 0.1	0.36 ± 0.13
PPN	0.02 ± 0.01	0.02 ± 0.01	0.04 ± 0.02
NO	0.01 ± 0.01	0.01 ± 0.01	0.02 ± 0.01
NO_2	0.03 ± 0.04	0.03 ± 0.03	0.03 ± 0.03
CO_2[b]	377.8 ± 1	377.8 ± 1	378.9 ± 1
H_2SO_4[c]	2.0 ± 2.6	2 ± 1	5 ± 10
Acetonitrile	0.21 ± 0.09	0.21 ± 0.09	0.31 ± 0.1
Methanol	0.91 ± 0.33	0.88 ± 0.3	1.5 ± 0.5
Acetone	0.91 ± 0.24	0.89 ± 0.2	1.4 ± 0.3
Benzene	0.03 ± 0.05	0.03 ± 0.05	0.1 ± 0.1
Toluene	0.01 ± 0.02	0.01 ± 0.02	0.02 ± 0.02
Propane	0.15 ± 0.1	0.13 ± 0.08	0.3 ± 0.2
Ethane	1.1 ± 0.3	1.06 ± 0.02	1.6 ± 0.3
Number of CO points	150,539	140,188	10,351
Number of WAS samples	429	401	28

[a] Average ±1σ. Values are given in ppbv except where noted. Propane and ethane data are from the WAS canisters.
[b] In ppmv.
[c] In 10^6 molecules/cm^3.

[24] The statistical filters previously described to separate transport data from background data require knowledge of the mean background levels of the tracer species. Using the CO data from Table 1, we can evaluate how our filter, based on the distinctly different populations (Figure 1) used for this study, compares to the previous long-range transport filters in the literature. *Talbot et al.* [1997] define enhancement as a species' mixing ratio greater than 2σ above the mean background level. In their analysis of the PEM West B data set, the mean background mixing ratio was determined using the smallest third of the measurements for a given altitude bin. Transport plumes were not removed from this data set before the averaging was performed, which could artificially increase the resulting background value. If this analysis were applied to the ITCT 2K2 data set, the mean background CO level would decrease from 120 ppbv to 110 ± 10 ppbv. Furthermore, if transport were defined as 2σ above the mean background level, in this instance the minimum CO mixing ratio used to distinguish transport plumes from the background would be 130 ppbv. 130 ppbv lies on the background marine FT CO distribution (Figure 1) observed during ITCT 2K2 and is not indicative of a clear enhancement. If we were to apply a similar 2σ definition to the mean marine FT CO mixing ratio (Table 1) without removing the transport plumes, the minimum transport CO mixing ratio would become 170 ppbv. 170 ppbv lies on enhanced marine FT CO distribution (Figure 1) observed

Table 2. Transport Statistics[a]

Species	29 April	5 May	6 May	10 May	11 May	13 May	17 May
CO	154 ± 5	211 ± 40	159 ± 6	198 ± 46	165 ± 15	170 ± 11	198 ± 27
O_3	51 ± 7	67 ± 3	73 ± 3	89 ± 13	72 ± 5	75 ± 8	84 ± 6
NO_y	0.37 ± 0.11	0.66 ± 0.14	0.53 ± 0.05	0.19 ± 0.21	0.51 ± 0.04	0.51 ± 0.09	0.63 ± 0.14
HNO_3	0.02 ± 0.04	0.03 ± 0.05	0 ± 0.04	0.04 ± 0.06	0.11 ± 0.07	0.02 ± 0.07	0.36 ± 0.19
PAN	0.21 ± 0.08	0.42 ± 0.10	0.36 ± 0.05	0.48 ± 0.10	NA	0.29 ± 0.04	0.09 ± 0.06
PPN	0.03 ± 0.01	0.04 ± 0.02	0.04 ± 0.01	0.06 ± 0.02	NA	0.03 ± 0.01	0.01 ± 0.01
NO	0.01 ± 0.01	0.01 ± 0.01	0.02 ± 0.02	0.03 ± 0.01	0 ± 0.01	NA	0.02 ± 0.01
NO_2	0.04 ± 0.04	0.03 ± 0.03	0.04 ± 0.03	0.08 ± 0.04	0.02 ± 0.03	NA	NA
CO_2[b]	378.3 ± 0.3	379.6 ± 0.4	378.6 ± 0.3	378.4 ± 0.7	379.2 ± 0.9	379.5 ± 0.3	379.9 ± 0.5
H_2SO_4[c]	4 ± 2	1 ± 7	NA	2 ± 1	1.3 ± 0.5	2 ± 1	16 ± 10
Acetonitrile	0.14 ± 0.05	0.37 ± 0.10	NA	0.22 ± 0.06	0.17 ± 0.03	0.29 ± 0.04	0.18 ± 0.02
Methanol	0.83 ± 0.33	1.7 ± 0.3	1.2 ± 0.3	1.3 ± 0.5	0.9 ± 0.2	1.2 ± 0.1	1.1 ± 0.2
Acetone	0.83 ± 0.21	1.5 ± 0.2	1.2 ± 0.2	1.4 ± 0.3	1.1 ± 0.1	1.1 ± 0.1	1.1 ± 0.1
Benzene	NA	0.09 ± 0.08	NA	0.2 ± 0.1	NA	0.05 ± 0.03	0.05 ± 0.02
Toluene	NA	NA	NA	NA	NA	0.03 ± 0.03	0.02 ± 0.01
Propane	0.35 ± 0.02	0.4 ± 0.3	0.3 ± 0.05	0.5 ± 0.1	NA	0.385	0.26 ± 0.08
Ethane	1.64 ± 0.07	1.6 ± 0.4	1.4 ± 0.2	1.8 ± 0.4	NA	1.461	1.5 ± 0.2
Alkyl nitrates	0.025 ± 0.004	0.018 ± 0.008	0.011 ± 0.001	0.017 ± 0.008	NA	.012	0.011 ± 0.002
Number of CO points	2417	3869	936	1408	208	502	972
Number of WAS samples	8	10	5	4	0	1	8

[a]Average ±1σ. Values are given in ppbv except where noted. NA, not measured during the transport plume. Propane, ethane, and alkyl nitrate data are from the WAS canisters. The total number of CO points from Table 2 is less than that shown in Table 1 because of encounters of transport on other days that are too short to analyze.
[b]In ppmv.
[c]In 10^6 molecules/cm^3.

during ITCT 2K2 but would exclude part of that distribution. The method used to determine the mean background level affects which transport plumes are or are not included in any analysis. This is important to realize when comparing the results of different analyses in the literature. The use of the cumulative distribution analysis, as shown in Figure 1, provides a more objective means to distinguish transport plumes from the background atmosphere than back trajectory analysis alone.

[25] Using the criteria described in section 2.2, Asian transport plumes were encountered on 7 of the 13 flights during ITCT 2K2: 29 April and 5, 6, 10, 11, 13, and 17 May. As mentioned earlier, the 13 May flight was primarily an urban air quality study over Los Angeles; however, a transport plume was encountered at 7.5 km along the coast between Monterey and Los Angeles. Table 2 presents a summary of the gas-phase observations within each plume. A range of average CO mixing ratios was observed in the different transport plumes. On the basis of the average CO mixing ratio observed within the transport plumes, the transport events are divided into "high-CO" (average CO mixing ratio $\geq$ 200 ppbv) and "low-CO" (average CO mixing ratio between 150 and 200 ppbv) transport plumes. In the following section, the relationships between NOy, O_3, and HNO_3 and CO are examined. In addition, the "high-CO" Asian transport plumes encountered during ITCT 2K2 on 5, 10, and 17 May are further characterized by the complete set of available gas-phase observations. The plumes encountered on these days exhibit important differences that illustrate the variability in Asian transport plumes.

3.2. Relationship Between Transport Trace Gases

[26] The 1-s marine FT NOy, O_3, and HNO_3 data are plotted versus the 1-s CO data in Figures 2, 3, and 4, respectively. In each figure the marine FT background data are shown as gray dots while the colored data represent different identifiable populations, i.e., stratospheric influence, lightning influence, and transport. In each, the stratosphere-influenced data are identified by the characteristic anticorrelation of NOy, O_3, and HNO_3 with CO [*Fischer et al.*, 2000]. In addition to the characteristic relationships with CO, the stratosphere-influenced data were also identified by low water mixing ratios. NOy is composed mainly of HNO_3 in this population. The population in purple identified as lightning influenced, from the 15 May

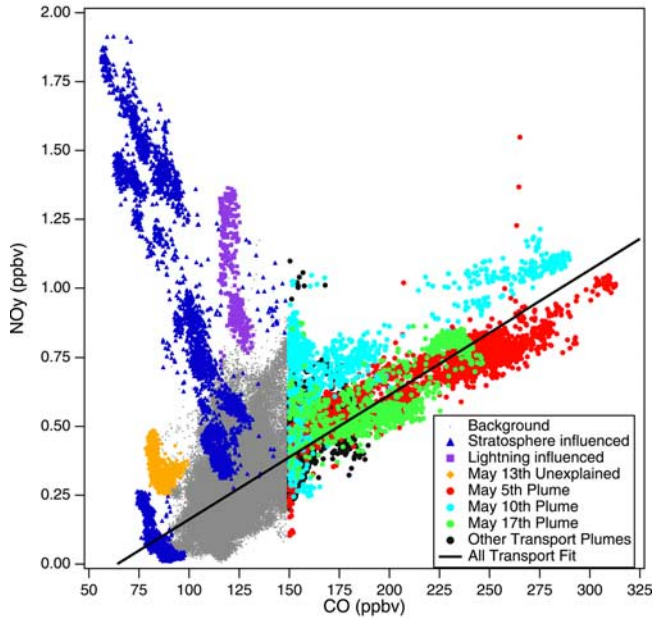

Figure 2. One-second NOy observations plotted against 1-s CO observations. A weighted, bivariate regression analysis on all the transport data yields a slope of (4.52 ± 0.02) × 10^{-3} with r^2 = 0.53.

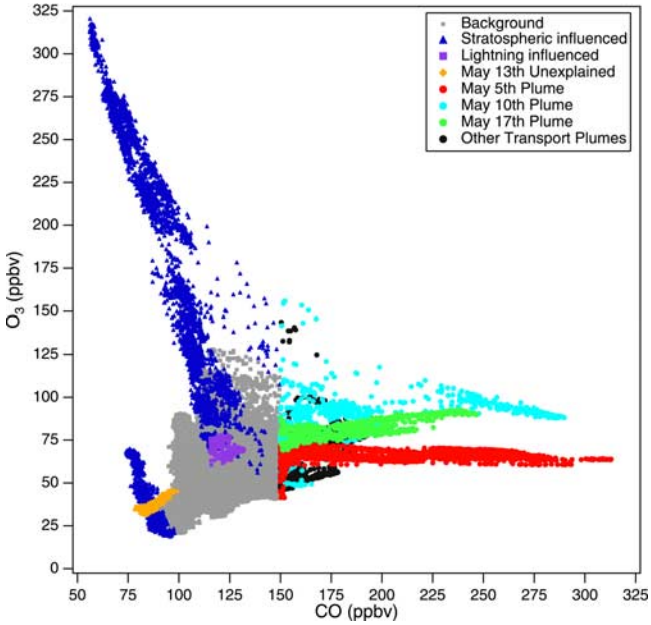

Figure 3. One-second O_3 observations plotted against 1-s CO observations.

flight, is unique in the ITCT 2K2 data because NOy increases while all other available gas-phase species (HNO_3 was not measured on this flight) remain unchanged. No substantial enhancement was observed in hydrocarbon levels and their characteristic ratios suggest an aged air mass. Because no corresponding increase in NOx or particles was seen and CO mixing ratios were around 120 ppbv, we speculate this population of data resulted from prior NOx production by lightning and subsequent photochemical oxidation over a period of days and not stratospheric influence, a transport plume, or an aircraft plume. The population in orange, from the 13 May flight, is interesting because, while the NOy/CO and HNO_3/CO relationships resemble stratosphere-influenced air, O_3 is correlated with CO indicating this is not a stratosphere-influenced population. The cause for the observed relationships on 13 May has not been determined.

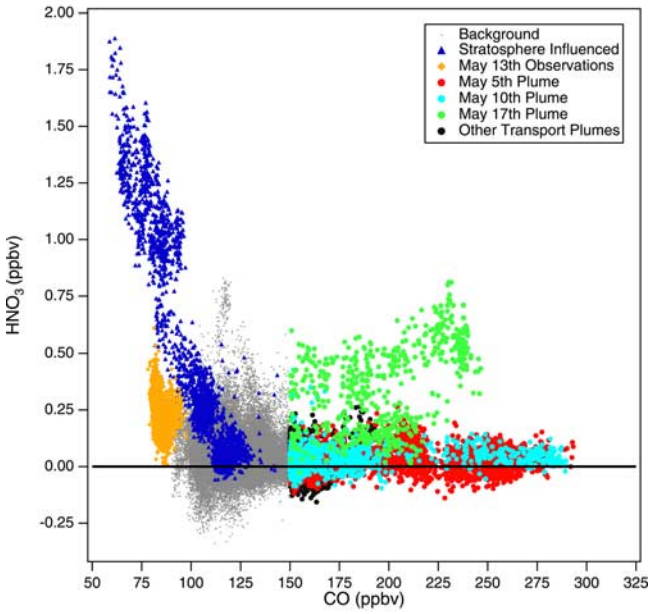

Figure 4. One-second HNO_3 observations plotted against 1-s CO observations. No lightning-influenced data are shown because HNO_3 observations were not made on that flight.

Table 3. NOy/CO Weighted Bivariate Regression Statistics

	Slope, ppbv/ppbv × 10^{-3}	r^2
All transport	4.52 ± 0.02	0.53
5 May	3.57 ± 0.03	0.92
10 May	4.97 ± 0.09	0.68
17 May	4.02 ± 0.10	0.80

[27] In each figure the data from the transport plumes is shown by date of flight for the three "high-CO" plumes, 5, 10, and 17 May, while the "low-CO" plumes have been grouped together in a single category labeled other transport plumes. A sharp line appears in the data at 150 ppbv CO denoting the selected lower limit for transport plume identification. From these figures a comparison of the transport plume data with the background data can be made.

[28] In the transport plumes NOy is always positively correlated with CO. A weighted, bivariate regression analysis was performed for plumes on 5, 10, and 17 May, and for a composite plume (not shown in Figures 2, 3, and 4) that included all transport plume data from ITCT. The weighting was set at $1/\sigma^2$ where σ is the estimated uncertainty of each measurement, as given in section 2.1. These results are summarized in Table 3. For the composite plume, NOy is correlated with CO (r^2 = 0.53) with a slope of (4.52 ± 0.02) × 10^{-3} ppbv/ppbv. Individually, each of the "high-CO" plumes on 5, 10, and 17 May, also show similar NOy/CO relationships with a high degree of correlation.

[29] The same is not seen in the O_3/CO relationship (Figure 3). The same weighted, bivariate regression analysis was performed on the O_3 and CO plume data, and these results are summarized in Table 4. For the composite plume O_3 is not correlated with CO (r^2 = 0.08). Unlike NOy, which showed a similar relationship to CO in all three "high-CO" plumes, O_3 has a different relationship in each. The 5 May event showed no correlation between O_3 and CO (r^2 = 0.00), whereas on 17 May, O_3 and CO are well correlated (r^2 = 0.70). O_3 was also slightly correlated with CO (r^2 = 0.24) in the 10 May plume, but this relationship is complicated by mixing with stratospheric air [*Cooper et al.*, 2004b].

[30] Within the transport plumes HNO_3 mixing ratios were typically below 100 pptv (Figure 4), except for a period on the 17 May flight. For the composite plume HNO_3, similar to O_3, was not correlated with CO (r^2 = 0.02). Also, no correlation between HNO_3 and CO was observed in the

Table 4. O_3/CO Weighted Bivariate Regression Statistics

	Slope, ppbv/ppbv	r^2
All transport	0.1 ± .008	0.08
5 May	0.004 ± 0.007	0.00
10 May	0.6 ± 0.1	0.24
17 May	0.2 ± 0.03	0.70

plumes on 5 May (r^2 = 0.00) or 10 May (r^2 = 0.01). However, a slight positive correlation (r^2 = 0.22) was observed in the plume on 17 May. The individual plumes are examined in greater detail below in order to explore the different relationships between the transported species.

3.3. The 5 May Plume

[31] On 5 May the NOAA WP-3D intercepted a "high-CO" Asian transport plume whose location had been broadly predicted by chemical transport models [*Forster et al.*, 2004]. This transport plume was observed between 33° and 37°N around 123°W in an altitude band of 5–8 km (Figures 5a and 5b). CO levels peaked at 313 ppbv making this the most concentrated transport plume, in terms of CO, seen during ITCT 2K2. Propane also shows strong enhancement but only in the lower section (5.5–6.5 km) of the enhanced CO altitude band. This suggests there may have been multiple transport layers present from different sources [*de Gouw et al.*, 2004; *Brock et al.*, 2004]. A detailed analysis of the meteorology associated with this transport plume is given by *Cooper et al.* [2004a], so only a brief description is given here. This Asian pollution plume was transported through two warm conveyor belts (WCBs) that had developed over Asia and the eastern Pacific. As seen in the back trajectories (Figures 5c and 5d), the WCBs brought the plume from the eastern coast of Asia northward over the Aleutian Islands of Alaska and then southward toward the west coast of North America. Once lifted into the free troposphere, this plume was transported at altitudes greater than 4 km.

[32] Time series plots of gas-phase species observed during two intersections of this plume are presented in Figure 6. Since equivalent potential temperature, θ_e, is conserved for both dry and saturated adiabatic processes [*Wallace and Hobbs*, 1977], it is used here as an additional tracer for plume identification. The "high-CO" plume observations were on similar equivalent potential temperature surfaces. During the periods of the "high-CO" plume shown, NOy was strongly correlated with CO (r^2 = 0.90), while O_3 was not (r^2 = 0.02). On average in this plume PAN accounted for 65% of the measured NOy. The observed NO, NO_2, and HNO_3 levels were low and showed no structure corresponding to that seen in CO or NOy. The sum of the individually measured NOy species (NO, NO_2, HNO_3, PAN, and PPN) for coincident measurements accounted for 85% of the measured NOy. As noted in section 2.1, the conversion efficiency of the NOy instrument for nitrate aerosol is uncharacterized. However, for the marine ITCT data set 90% of the aerosol nitrate as measured by the PILS instrument was equivalent to 0.035 ppbv or less [*Brock et al.*, 2004]. So, even if 100% were converted to NOy on average it would account for only a few percent of the measured NOy in the plumes discussed here. The PPN/PAN ratio of 0.15 was also enhanced in the plume compared to 0.08 in the background.

[33] Of all the VOCs measured acetone and methanol showed the largest and most consistent enhancements in the transport plumes (Table 2). Though the primary atmospheric sources of each are biogenic, anthropogenic emissions and biomass burning sources are nonnegligible. Combined direct anthropogenic emissions, biomass burning, and oxidation of other anthropogenic emissions may account for up to 25% and 10% of the atmospheric source for acetone and methanol, respectively [*Jacob et al.*, 2002; *Heikes et al.*, 2002]. Acetone and methanol have lifetimes of 15 days [*Jacob et al.*, 2002] and 9 days [*Heikes et al.*, 2002] respectively, and thus are long-lived enough for transpacific transport. Similarly, propane and ethane both have anthropogenic (mainly industrial) and biomass burning sources and lifetimes long enough for intercontinental transport [*Parrish et al.*, 1992], and enhancements were observed in the transport plumes (Figure 6). The low mixing ratios of HNO_3 and H_2SO_4 suggest that this plume had undergone cloud processing during transport, consistent with the meteorological analysis reported by *Cooper et al.* [2004a]. This coupled with enhanced levels of PAN and no enhancement in submicron particle volume or water-soluble ionic particulate compounds, such as nitrate or sulfate [*Brock et al.*, 2004], also suggests that there was no further PAN decomposition to NOx or SO_2 oxidation to H_2SO_4 since cloud processing.

3.4. The 10 May Plume

[34] The "high-CO" Asian transport plume observed on 10 May (Figure 7a) had generally similar chemical characteristics to the plume observed on the 5 May. The high average CO mixing ratio on this flight was due to two separate layers (Figure 7b). Enhancements in propane were coincident with the "high-CO" transport layers. Another feature observed on 10 May was high mixing ratios of O_3 associated with stratospheric air. The highest O_3 levels were seen between 5.5 and 6 km and 3.5 and 4.5 km. Evident in Figure 7b is the extremely close vertical spacing between stratospheric air and the Asian pollution plume. The 10 May plume was transported through a WCB, like the 5 May plume; however, on 10 May, stratospheric air was also mixed into the plume. Because of the complexity of mixing, it is difficult to ascertain how much stratospheric air was mixed into the plume [*Cooper et al.*, 2004b]. Back trajectory analysis suggests this plume was transported along the Pacific Rim but much further north than the plume on 5 May (Figure 7c). The trajectory analysis indicates this plume was transported at similar altitudes to the plume on the 5 May (Figure 7d). However, in this case, the trajectories had trouble distinguishing between the decaying WCB and the stratospheric intrusion; thus none of the trajectories shown reach the surface.

[35] The data show evidence of intermingling of stratosphere-influenced air and the pollution plume. In Figure 8, the time axis is broken to show the two "high-CO" plumes, shaded in beige, and periods of stratospheric influence, shaded in blue, in more detail. The high-CO layers were observed along the same θ_e surface, while a "low-CO" transport layer, at 2109 UT, was on a different θ_e surface. This was true for other "low-CO" transport layers observed on this flight not shown in the time series. Different CO mixing ratios observed on different θ_e surfaces suggests the possibility that two or more distinct transport plumes were sampled on this flight. The "low-CO" transport layer at 2109 UT was observed for a short time period. A difficulty in analyzing these short intersections is that many important, but less frequent, measurements, such as PAN or WAS canister data, are not available to enable a full detailed analysis.

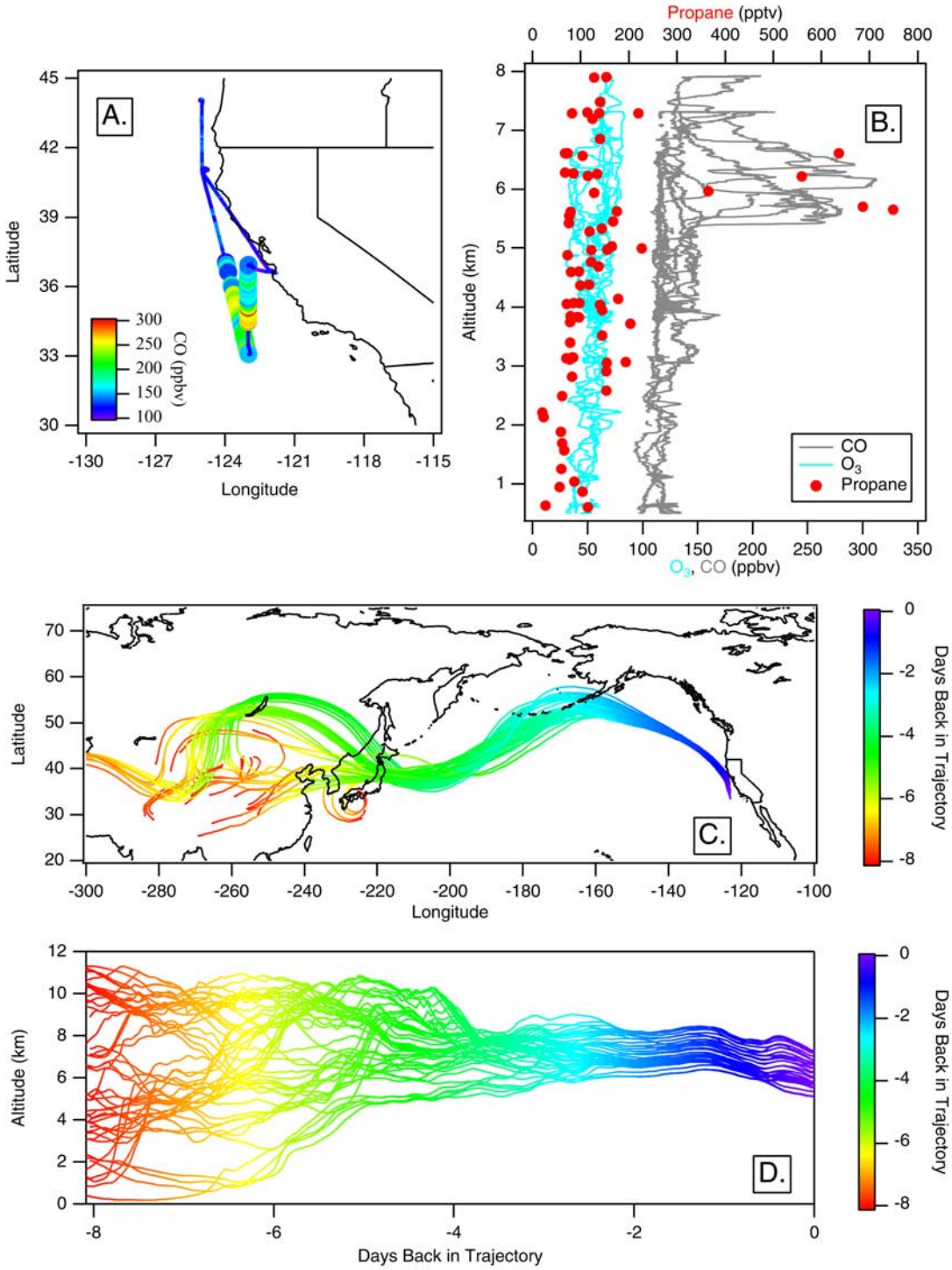

Figure 5. (a) The 5 May flight track colored by the 1-s CO observations with the large markers, indicating the intersection of the transport plume. (b) Altitude (km) versus O_3 (teal) and CO (gray) on the bottom axis and propane (red circles) on the top axis above 0.5 km for the whole flight. (c) The 8-day back trajectories associated with the intersected plume colored by the number of days back along the trajectory. (d) Altitude of the back trajectories.

[36] From 2045 to 2057 UT, CO mixing ratios varied from 110 to 125 ppbv. For this same time period O_3, NOy, and PAN mixing ratios were enhanced from 2050 through 2057 UT, while HNO_3 mixing ratios remained low. No anticorrelation between NOy and CO or HNO_3 and CO coupled with an enhancement of PAN suggests this was not stratospheric air. From 2057 to 2058 UT (blue shading) O_3, NOy, and HNO_3 were anticorrelated with CO indicating stratospheric air. From 2058 to 2100 UT (beige shading) CO and NOy were correlated indicating an Asian

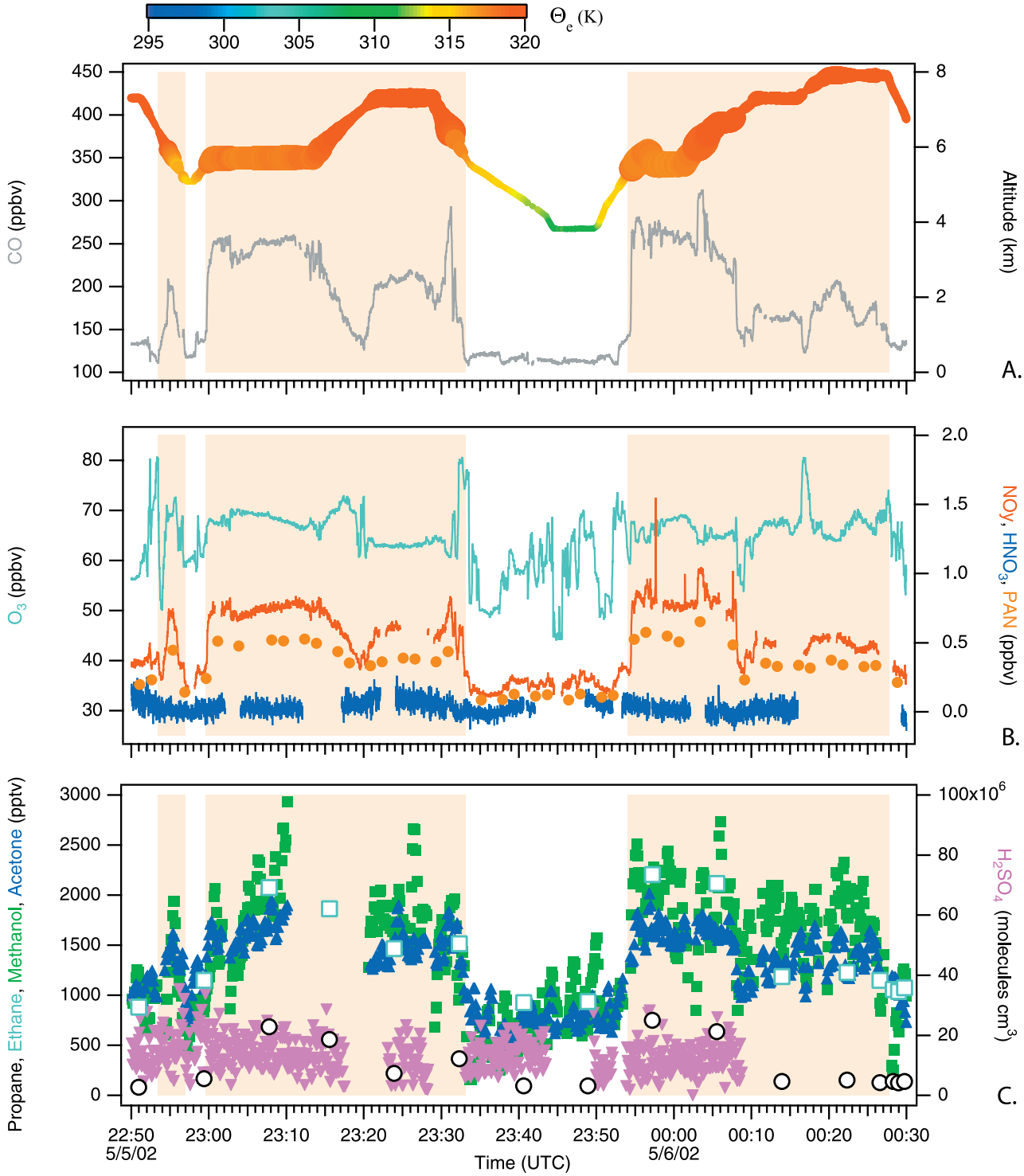

Figure 6. Time series from the 5 May flight for the photochemically important gas-phase species and others that show enhancement in the transport plume. Transport plumes are shaded in beige. (a) CO (gray) plotted on the left axis and altitude colored by equivalent potential temperature and sized by CO mixing ratio plotted on the right axis. (b) O_3 (teal) plotted on the left axis and NOy (red), HNO_3 (blue), and PAN (orange circles) plotted on the right axis. NO, NO_2, and PPN mixing ratios are on average less than 0.050 ppbv and therefore not shown. (c) Acetone (blue triangles), methanol (green squares), propane (open black circles), and ethane (open teal squares) plotted on the left axis in pptv and H_2SO_4 (upside-down pink triangles) plotted on the right axis in molecules cm^{-3}.

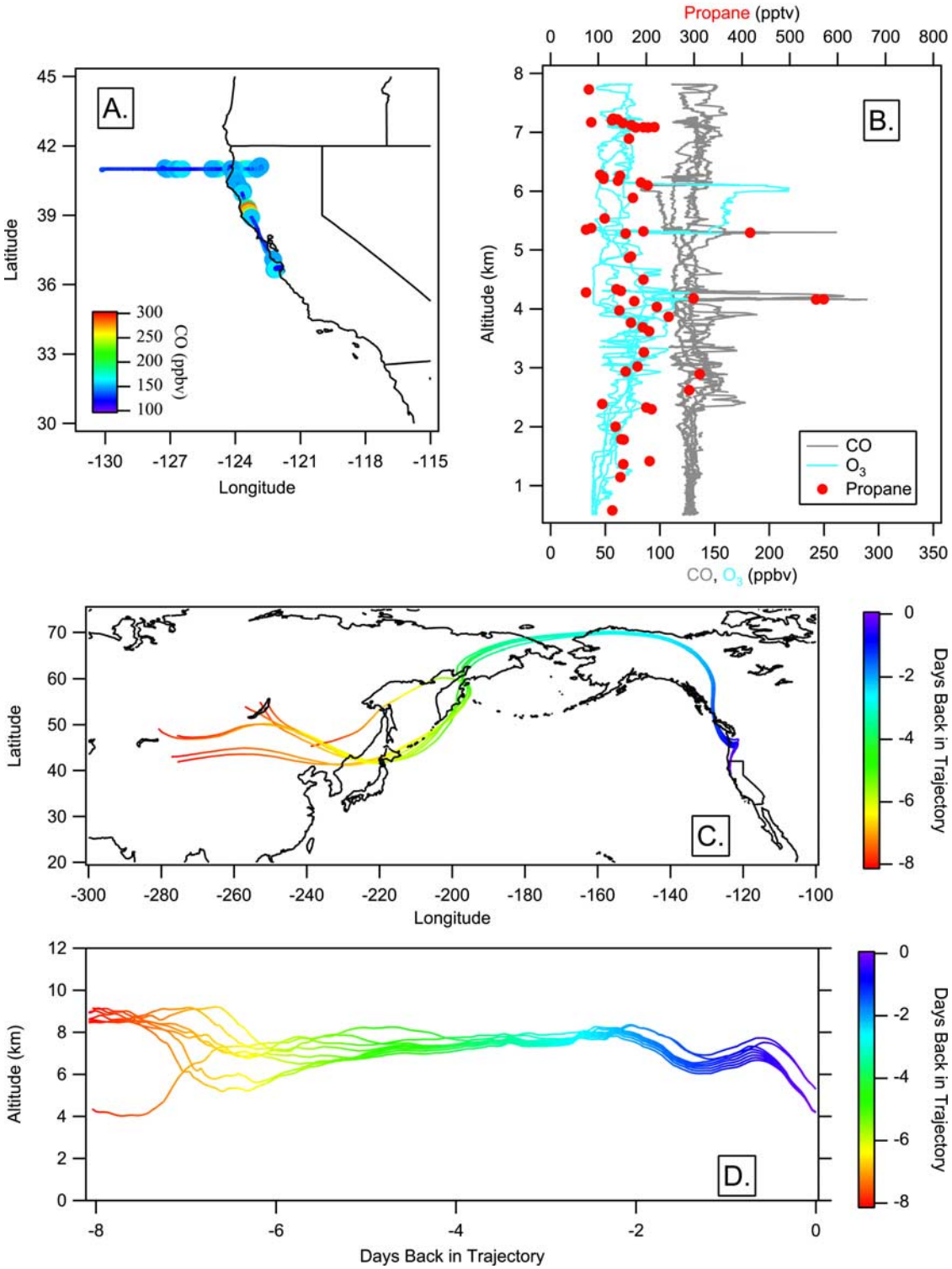

Figure 7. (a) The 10 May flight track colored by the 1-s CO observations with the large markers, indicating intersection of the transport plume. (b) Altitude (km) versus O_3 (teal) and CO (gray) on the bottom axis and propane (red circles) on the top axis above 0.5 km for the whole flight. (c) The 8-day back trajectories associated with intersected plume colored by the number of days back along the trajectory. (d) Altitude of the back trajectories.

transport plume. At 2100 UT (blue shading) O_3 and CO were anticorrelated indicating an abrupt change back to stratosphere-influenced air. The rest of the time series shows O_3, NOy, and HNO_3 anticorrelated with CO at low levels (~100 ppbv), indicating a transition back into stratospherically influenced air. The highest mixing ratios of O_3, NOy, and HNO_3 were seen from 2107 to 2108 UT (blue shading) and were coincident with the lowest CO

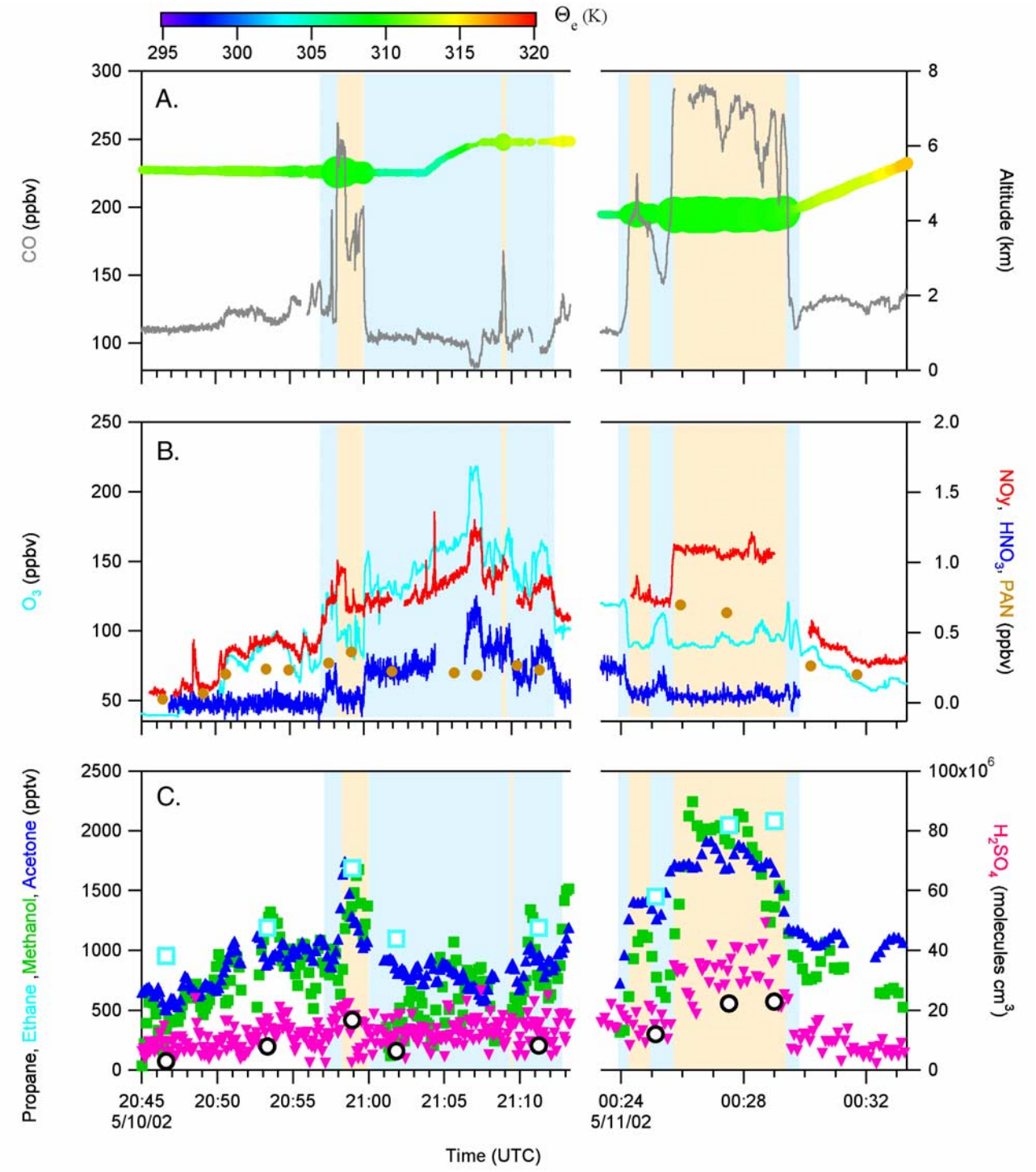

Figure 8. Time series from the 10 May flight for the photochemically important gas-phase species and others that show enhancement in the transport plume. Transport plumes are shaded in peach. Stratosphere-influenced periods are shaded in blue. Note the time break in the *x* axis. (a) CO (gray) plotted on the left axis and altitude colored by equivalent potential temperature and sized by CO mixing ratio plotted on the right axis. (b) O_3 (teal) plotted on the left axis and NOy (red), HNO_3 (blue), and PAN (orange circles). NO, NO_2, and PPN mixing ratios are on average less than 0.050 ppbv and therefore not shown. (c) Acetone (blue triangles), methanol (green squares), propane (open black circles), and ethane (open teal squares) plotted on the left axis in pptv and H_2SO_4 (upside-down pink triangles) plotted on the right axis in molecules cm^{-3}.

observations, ~85 ppbv, indicating this was the most concentrated period of stratospheric influence. Another period of high O_3/CO anticorrelation was observed from 2111 to 2113 UT, and serves as a good example of fine-scale intermingling of stratospheric air and an Asian emission plume. We also see that because NOy was enhanced in both the intrusion and pollution plume, it does not uniquely identify the source of either air mass.

[37] The second encounter of the plume, from 0024 to 0029 UT, did not involve as much fine-scale intermingling. This was a 5-min-long intercept of the plume with clear evidence of stratospheric mixing at 0025 UT (blue shading) where CO was anticorrelated with both O_3 and HNO_3. Though NOy showed no structure, interpretation is difficult because of its enhancement in both stratospheric air and Asian emission plumes. As in the transport plume on 5 May, PAN accounted for ~65% of measured NOy with very low mixing ratios of NO, NO_2, and HNO_3 observed in the transport plume. The sum of the individually measured NOy species (NO, NO_2, HNO_3, PAN, and PPN) accounted for 88% of the measured NOy in the plume on 10 May. This is comparable to the observations on 5 May, though there are fewer coincident measurements of the nitrogen species for comparison. The alkyl nitrates were also elevated in the plume and account for 4% of measured NOy. Similar to 5 May, the PPN/PAN ratio on 10 May was enhanced in the plume, approximately 0.13, compared to 0.09 outside.

[38] Acetone, methanol, propane, and ethane each showed enhancements corresponding to the "high-CO" transport plume. The enhancement in each was greater in the second plume intersection (0024–0029 UT) than in the first (2058–2100 UT). H_2SO_4 was not clearly enhanced in the first intersection, but definitely was enhanced in the second. HNO_3 mixing ratios were low, even though enhanced H_2SO_4 levels indicate no recent cloud processing had occurred. Typically, lower mixing ratios of acetone, methanol, propane, and ethane were observed in the stratospherically influenced air than in the plume.

3.5. The 17 May Plume

[39] Significantly different gas-phase chemical characteristics were observed in the 17 May "high-CO" Asian transport then in the previous plumes. This transport plume was intersected at four locations on 17 May from 31° to 37°N and 129° to 121°W (Figure 9a). The transport plume was also observed at lower altitudes, 2–4 km, than on the previous flights (Figure 9b). Positive correlations between the CO and O_3 vertical structures were also observed with propane enhancement in the "high-CO" transport layers. Unlike the plumes observed on 5 and 10 May, the 8-day back trajectories (Figures 9c and 9d) from 17 May do not extend to the Asian continent. They do indicate that for the last 8 days this plume took a more southerly route across the central North Pacific, slowly descending along the way. Longer trajectory calculations suggest that the air parcels associated with the plume were transported from initial altitudes of 1–2 km over eastern Asia on a timescale of 14 days [*Brock et al.*, 2004].

[40] In Figure 10, the time series is broken to show the plume encounters in more detail. All except the first encounter at 1950 UT were on a similar θ_e surface that decreased in altitude along the flight track. In encounters on this θ_e surface O_3, NOy, and HNO_3 were positively correlated with CO with r^2 values of 0.76, 0.77, and 0.65, respectively. The time series shows the NOy partitioning changing along the last three plume intersections. Each successive intersection was made at a lower altitude and at higher ambient temperature. During the 2136 UT intersection, PAN and HNO_3 mixing ratios were nearly equal and each accounted for 30% of the measured NOy. In the next two intersections, on the other hand, HNO_3 mixing ratios were higher than those of PAN and accounted for 80–90% of the measured NOy. This is a significant shift in NOy partitioning from the previous transport plumes where PAN mixing ratios were much greater than HNO_3, with PAN accounting for 60–70% of measured NOy. Because of lack of NO_2 and J_{NO2} observations during these plume intersects, a NOy budget calculation cannot be made for the 17 May plume as was done for the 5 May and 10 May plumes. The contribution of alkyl nitrates to the measured NOy was much lower than in the previous plumes. The alkyl nitrates contributed only 0.5% to the measured NOy, compared to 4–6% on 5 and 10 May. The PPN/PAN ratio in the plume was 0.15, similar to that observed in the previous transport plumes, and greater than the 0.09 observed in the marine background data on 17 May.

[41] Acetone, methanol, propane, and ethane each showed enhancements corresponding to CO in the last three plume intersections, further evidence that this was an anthropogenic pollution plume. In the plume intersection at 2233 UT, SO_2 mixing ratios (not shown) of 0.55 ppbv, detectable above instrumental noise, were observed. H_2SO_4 also showed enhancements corresponding to the CO in these plume sections. The high mixing ratios of both HNO_3 and H_2SO_4 observed during the transport suggest that it has been on the order of ~7 days since this plume had undergone cloud processing [*Brock et al.*, 2004].

[42] As mentioned earlier, the first intersection of Asian transport on this flight at 1950 UT was on a different θ_e surface than the others. At 1950 UT CO, O_3, and NOy on this θ_e surface (~315 K) showed an enhancement that lasted approximately 2 min. Outside of the plume, from 1953 to 1958 UT, O_3, NOy, HNO_3, and PAN each remained enhanced. Earlier from 1945 to 1950 UT θ_e was similar to that in the plumes previously described, ~310 K, and no enhancement in any gas-phase species were seen. It appears that the air mass on the 315 K θ_e surface was enhanced in O_3, NOy, HNO_3, and PAN while that on the 310 K surface was not. Thus it is difficult to determine whether the "high-CO" plume at 1950 UT was a different plume than the others seen at the same equivalent potential temperature surface or if it was the same plume mixed into a different background air mass.

4. Discussion

[43] Distinguishable from the background CO distribution in the FT over the temperate North Pacific were Asian emission plumes in which CO mixing ratios exceeded 150 ppbv. These plumes were also characterized by corresponding enhancements in NOy species, acetone, methanol, propane, and ethane concentrations. However, enhancements in O_3, PAN, HNO_3, or H_2SO_4 were observed in only some plumes. Similar slopes of NOy/CO were also

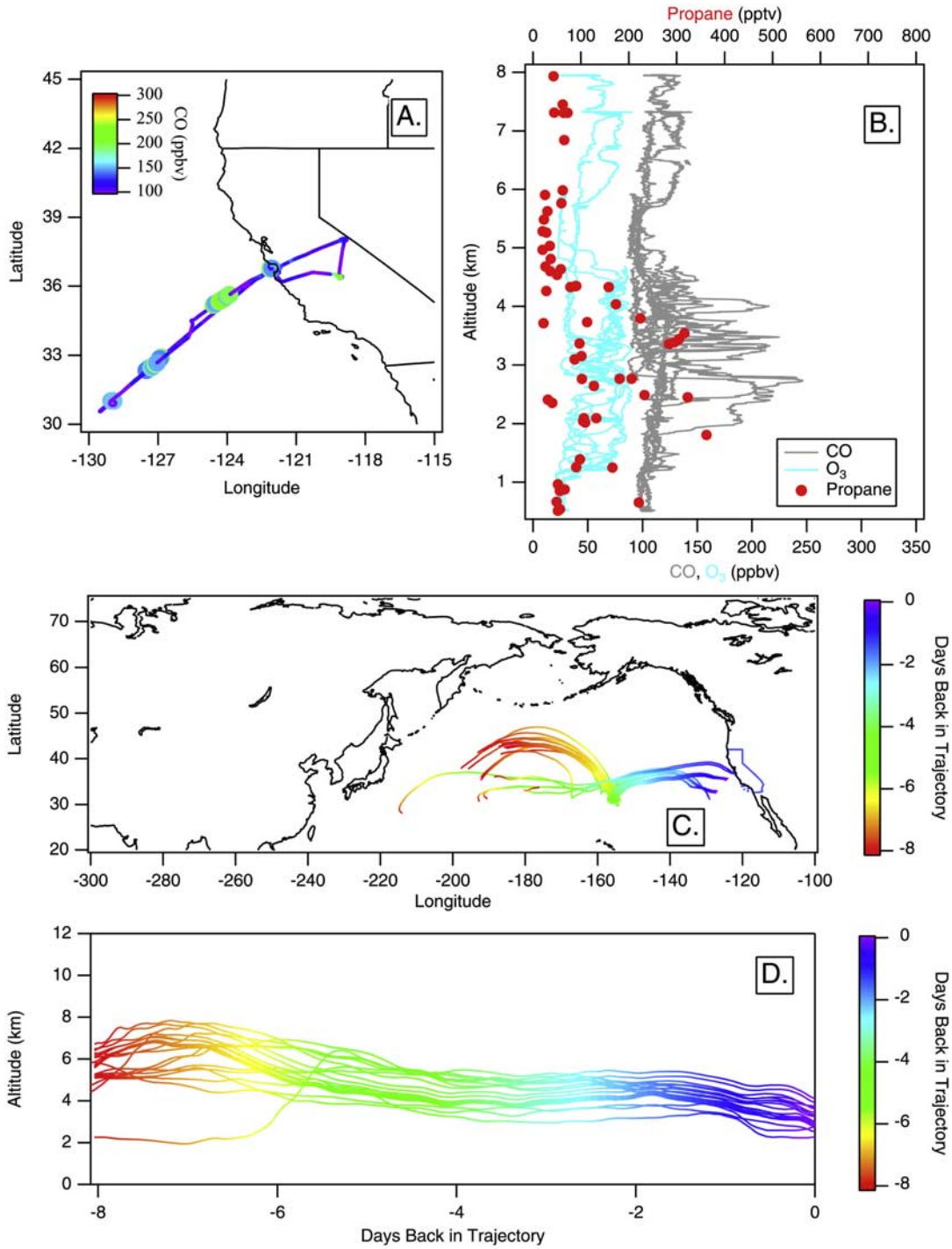

Figure 9. (a) The 17 May flight track colored by the 1-s CO observations with the large markers, indicating intersection of the transport plume. (b) Altitude (km) versus O_3 (teal) and CO (gray) on the bottom axis and propane (red circles) on the top axis above 0.5 km for the whole flight. (c) The 8-day back trajectories associated with intersected plume colored by the number of days back along the trajectory. (d) Altitude of the back trajectories.

observed in each plume, though the partitioning between NOy species differed. Unlike the NOy/CO slopes, the O_3/CO slopes differed in each plume.

[44] Average NOy/CO emission ratios in Asia vary depending on country from 0.04 to 0.28 with an average of 0.06 [*Streets et al.*, 2003]. Since CO has a lifetime of approximately 30 days its concentration is not expected to change significantly on transpacific transport timescales. Thus comparison of observed NOy/CO ratios to the NOy/CO emission ratios in Asia gives information on

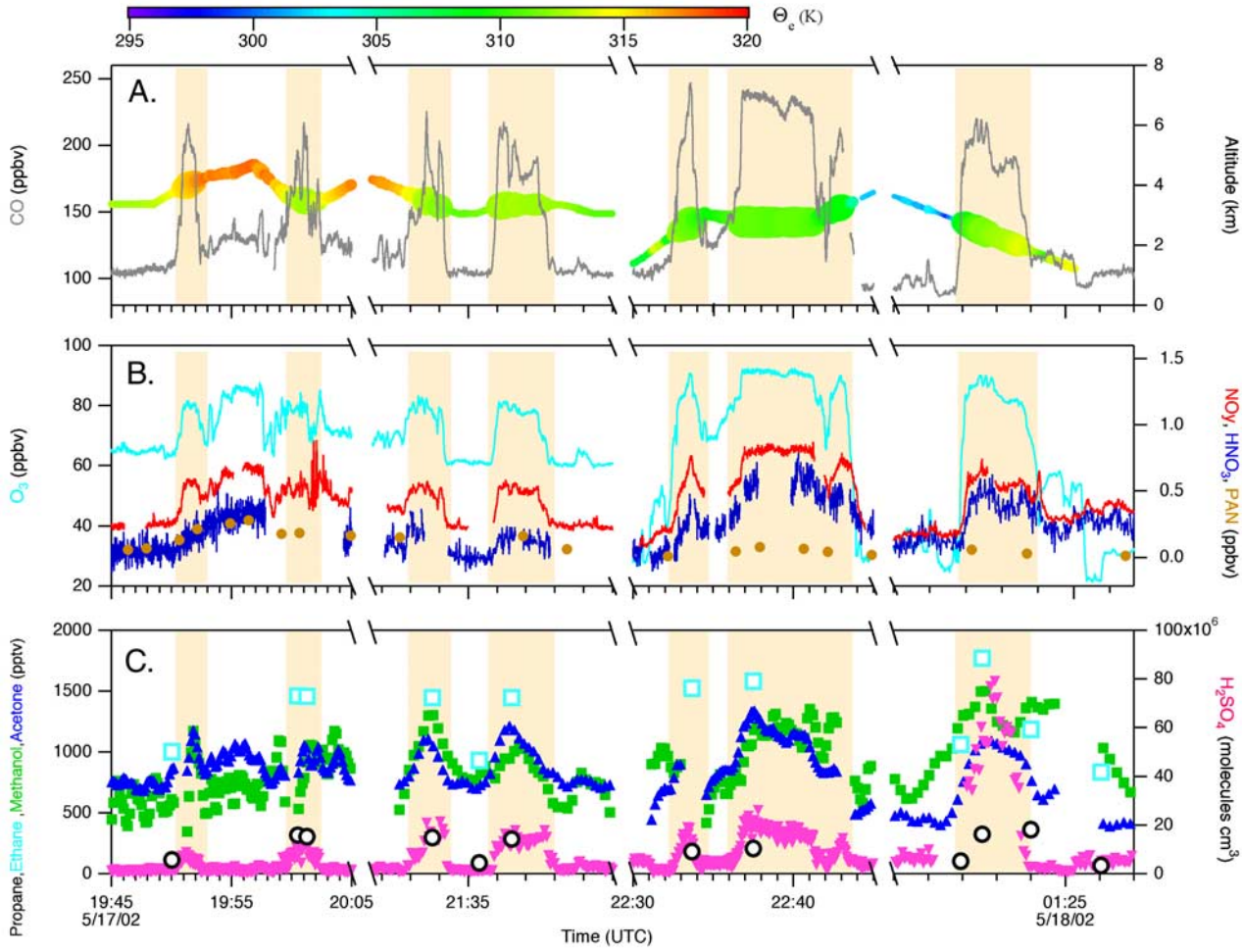

Figure 10. Time series from the 17 May flight for the photochemically important gas-phase species and others that show enhancement in the transport plume. Note the time break in the *x* axis. (a) CO (gray) plotted on the left axis and altitude colored by equivalent potential temperature and sized by CO mixing ratio plotted on the right axis. (b) O_3 (teal) plotted on the left axis and NOy (red), HNO_3 (blue), and PAN (orange circles) plotted on the right axis. NO and PPN mixing ratios are on average less than 0.050 ppbv and therefore not shown. NO_2 was not measured on this flight. (c) Acetone (blue triangles), methanol (green squares), propane (open black circles), and ethane (open teal squares) plotted on the left axis in pptv and H_2SO_4 (upside-down pink triangles) plotted on the right axis in molecules cm^{-3}.

the efficiency of NOy transport from source to receptor region. For the composite transport plume described earlier, the NOy/CO ratio was $(4.52 \pm 0.02) \times 10^{-3}$ ppbv/ppbv indicating that over 90% of the NOy had been removed during transport. The same is true for the NOy/CO ratio from each individual plume (Table 3). Observations made over east Asia indicate that only 10–20% of NOy emitted from the surface is transported through a WCB [*Miyazaki et al.*, 2003; *Koike et al.*, 2003]. Significant removal of anthropogenic NOy in the boundary layer (BL) before transport into the FT has been observed and modeled elsewhere [*Takegawa et al.*, 2003; *Stohl et al.*, 2002]. The Asian emission plume observations during ITCT 2K2 are consistent with the earlier findings that most of the NOy is removed near the source, and therefore not available for long-distance transport.

[45] Though similar amounts of NOy relative to CO were observed in each plume, the partitioning between the reactive nitrogen species differed substantially. For all the marine FT nitrogen data a weighted, bivariate fit, similar to that described in section 3.2, of the sum of NO, NO_2, HNO_3, PAN, and PPN against measured NOy yields a slope of 0.88 ± 0.03 with an intercept of -0.010 ppbv ($r^2 = 0.90$). Alkyl nitrates accounted for, on average, 1% of measured marine FT NOy. On the basis of the combined stated accuracies of the individual species, from section 2.1, the measured slope should lie within 1 ± 0.28 ppbv/ppbv, under the assumption that all of the individual reactive nitrogen species are measured. There are a few caveats with this approach. First, summing the stated accuracies in quadrature assumes equal weighting to each species and this is obviously not true in the atmosphere. Second, the instrumental precision, which has a greater affect on the total uncertainty at lower mixing ratios, is ignored. Nevertheless, 28% is a reasonable upper bound on the uncertainty of the sum of the individual reactive nitrogen species measured during ITCT

2K2. The sum of the individual reactive nitrogen species agrees with the measured NOy within the stated instrumental uncertainties. Since coincident measurements of the alkyl nitrates, PAN, and PPN are sparse; the alkyl nitrate data were left out of this uncertainty calculation.

[46] Observations in East Asia show that the dominant NOy species transported from the BL by a WCB is PAN [*Miyazaki et al.*, 2003]. The atmospheric lifetime of PAN is controlled by thermal decomposition (below 7 km) and photolysis (above 7 km) [*Talukdar et al.*, 1995]. With respect to thermal decomposition the lifetime of PAN is approximately 1 day at 4°C and 20 days at −12°C [*Roberts*, 1990]. Thus PAN is highly stable in the middle and upper troposphere and can be a mechanism for transporting NOx [*Singh et al.*, 1986]. PAN thermally decomposes into the acetyl peroxy radical and NO_2. NO_2 can react with the acetyl peroxy radical to reform PAN or be oxidized by the OH radical to form HNO_3. The importance of the thermal decomposition of PAN has been discussed for other transport events [*Kotchenruther et al.*, 2001b]. In the plumes discussed here NOy partitioning was largely controlled by the transport meteorology through ambient temperature. In the 5 and 10 May plumes, NOy consisted mostly of PAN, while in the 17 May plume, NOy was mainly HNO_3, at least at the lower altitude plume intersections. The plumes on 5 and 10 May were transported at higher latitudes and altitudes than the plume on 17 May. Consequently, the ambient temperatures calculated along the back trajectories were on average 20 to 30°C colder for the 5 and 10 May plumes than for the 17 May plume. The higher HNO_3/NOy ratio observed in the plume on 17 May is most likely the result of PAN decomposition during the descent of the air mass with subsequent NO_2 oxidation to HNO_3. During the transport of the 5 and 10 May plumes, the colder temperatures kept NOx in the PAN reservoir. Modeling results of NOy transport and partitioning agree [*Moxim et al.*, 1996; *Hess and Vukicevic*, 2003] qualitatively with the NOy partitioning as a function of transport meteorology observed during ITCT 2K2.

[47] A second difference in the NOy partitioning is the fraction of NOy observed in the form of measured alkyl nitrates. Though the sum of the measured alkyl nitrates was similar in each plume (Table 2), the observed alkyl nitrate/NOy ratio on 17 May differed from that on 5 and 10 May. In the transport plumes on 5 and 10 May, alkyl nitrates account for 6% and 4% of the measured NOy, respectively; whereas, on 17 May the alkyl nitrates accounted for less than 1% of the measured NOy. For the whole ITCT marine FT data set, the sum of alkyl nitrates accounted for 1% of measured NOy. The small contribution of alkyl nitrates to the measured NOy for the whole ITCT marine FT data is consistent with previous studies [*Flocke et al.*, 1991; *Ridley et al.*, 1997]. Unlike PAN, the primary atmospheric loss mechanisms for the alkyl nitrates are photolysis and reaction with OH, not thermal decomposition [*Roberts and Fajer*, 1989; *Clemitshaw et al.*, 1997; *Talukdar et al.*, 1997]. The enhanced alkyl nitrate/NOy ratios observed in the plumes on 5 and 10 May compared to 17 May and the ITCT marine FT data set as a whole can be explained by enhancements in the source region or a more photochemically active environment, such as higher OH levels or photolysis frequencies, within the plume on 17 May.

[48] In the "high-CO" transport plumes the PPN/PAN ratio was enhanced compared to the background marine FT. The enhanced ratio observed in the plumes is consistent with anthropogenic driven hydrocarbon chemistry [*Roberts et al.*, 1998]. A more detailed examination of PPN/PAN ratios and their relationship to different sources is given by J. M. Roberts et al. (Measurement of peroxycarboxylic nitric anhydrides (PANs) in intercontinental transport from Asia during ITCT 2K2, submitted to *Journal of Geophysical Research*, 2004).

[49] The observed O_3/CO relationships (Figure 3) are different in each of the three high-CO plumes, and we have not been able to definitively account for the relative contributions of several factors that determine these relationships. The outflow from ascending WCBs of midlatitude cyclones generates these plumes [*Cooper et al.*, 2004a]. These WCBs loft air from the continental boundary layer with O_3 and CO levels determined by the emissions, the photochemical production and loss, and the deposition processes in the source region. Small slopes (either positive or negative) generally characterize the O_3/CO relationships [*Parrish et al.*, 1998]. The O_3 and CO levels from the source region can then be modified during transport, primarily by dilution with background FT air and possibly O_3 production from NO_x-VOC photochemistry driven by PAN thermal decomposition. The O_3/CO relationship finally observed during aircraft sampling of a transported plume is a "mixing curve" that results from the aircraft passing from background FT air, into the plume, and then out into (perhaps different) background air. Only if the background FT air, both that responsible for dilution during transport and that adjacent to the plume at the time of sampling, has approximately the same O_3 and CO levels as the original background air in the continental boundary layer source region, can the observed O_3/CO relationships directly indicate the effect of the anthropogenic emissions upon the observed O_3 levels.

[50] A frequent confounding factor arises from the descending dry air (DA) stream within each cyclone that brings air with significant stratospheric influence down to the midtroposphere. A large negative slope (see blue triangles in Figure 3) characterizes the O_3/CO relationship in the DA. As these cyclones mature and then dissipate, the air in the WCB and the DA intermingle. As illustrated in Figures 6, 8, and 10 these airstreams often are at the same equivalent potential temperature, so there is no thermodynamic barrier to their mixing, and a complex intermingling of these air streams results [*Cooper et al.*, 2004b]. This intermingling complicates the simple interpretation of any observed O_3/CO relationship. For example, the O_3/CO relationship seen on 10 May was evidently dominated by the intermingling of stratospheric air with the pollution plume. On 5 and the 17 May the observed stratospheric influence was not as pronounced, but was likely still important. On 5 May the highest O_3 (up to 80 ppbv in Figure 6) in the vicinity of the plumes was seen immediately adjacent to the elevated CO, and on 17 May the highest O_3 seen in the first 20 min of plume encounters was seen between the two pronounced CO plumes (1953–1958 UT), and these O_3 levels were nearly as high as the maxima observed in the later plume encounters. The observed O_3/CO relationships from all three flights are likely affected by the mixing of anthropogenic and stratospheric influences.

[51] An attempt was made to quantitatively determine the anthropogenic and stratospheric contributions to the O_3 levels in each the three "high-CO" plumes observed. It was assumed that every 1-s measurement represented an air parcel that was a linear combination of air from a stratospheric intrusion, the marine troposphere background, and a concentrated anthropogenic plume. For each flight a multivariate, linear, least squares analysis (similar to factor analysis) was performed on the O_3, CO, CO_2, and NO_y data collected within the equivalent potential temperature range that included the plume. The best fit obtained for each of these three "high-CO" flights implied an O_3/CO ratio of 0.10–0.12 in the anthropogenic plumes. However, the confidence limits on these ratios were very wide, and satisfactory fits were found for O_3/CO ratios in the anthropogenic plume ranging from negative (indicating O_3 destruction due to anthropogenic effects) to positive values ($\approx$1) that are larger than have generally been observed in plumes of anthropogenic emissions. Thus we cannot determine if the observed O_3 enhancements associated with the anthropogenic plumes on 10 and 17 May were predominantly stratospheric or anthropogenic in origin. For example, the positive correlation evident in the 17 May data in Figure 2 indicates that the plume was enhanced in both CO and O_3. These enhancements could possibly be due to at least two different causes: (1) CO from anthropogenic emissions and O_3 from photochemical production in the source region or during transport, possibly NOx-VOC photochemistry initiated by the observed PAN thermal decomposition, and/or (2) CO from anthropogenic emissions and O_3 from the DA mixed into the WCB outflow. Similar considerations also apply to the other two flights.

5. Conclusions

[52] The methodology used here allowed unambiguous identification of Asian emission plumes from the background marine FT on the basis of CO observations. Three plumes with average CO mixing ratios 200 ppbv or greater were characterized by their measured gas-phase composition. Enhancements of NOy, PPN/PAN, acetone, methanol, and propane were observed in these plumes. Similar NOy/CO ratios were seen in each plume. Comparing the observed NOy/CO ratio with those reported from Asia indicates significant levels of NOy had been removed during transport. The partitioning of NOy differed according to the transport meteorology. NOy in plumes transported in colder regions (5 and 10 May) consisted mainly of PAN, while HNO_3 was the primary component of NOy in a plume transported in warmer regions (17 May). Alkyl nitrates (methyl-, 2-butyl-, pentyl, 2-pentyl-, 3-pentyl-, ethyl-, 1-propyl-, and 2-propyl nitrate) were found to contribute more to the NOy budget in plumes transported through colder regions, however, it is difficult to ascertain whether this reflects different source compositions or photochemistry in route. Unlike the NOy/CO relationship, the O_3/CO one was found to be different in each plume.

[53] This study illustrates the challenges associated with understanding O_3 pollution from long-range transport. The observed O_3/CO relationship in the receptor region is different in each plume with the possible causes including different sources, different mixing into background air, different O_3 loss and formation mechanisms during transport, or a combination of these. North American O_3 levels will be influenced by how much O_3 is directly transported and the levels of precursor species transported. The three plumes sampled provided examples of both direct O_3 transport, either formed in transport or unchanged from source, and transport of O_3 precursor species.

[54] **Acknowledgments.** The author, John B. Nowak, was supported by a National Research Council Research Associateship Award at the NOAA Aeronomy Laboratory. The authors thank M. Trainer, C. A. Brock, and D. T. Seuper for helpful discussions and manuscript suggestions. We also thank Verity Stroud, Kristen Johnson, and Nadege Schwaller for technical support of the WAS analyses. NCAR is operated by the University Corporation for Atmospheric Research under sponsorship of the National Science Foundation. This work was supported in part by the NOAA Health of the Atmosphere and Climate and Global Change Programs and the National Science Foundation. In particular, L. G. Huey acknowledges support from NA06GP0410.

References

Atlas, E., S. M. Schauffler, J. T. Merrill, C. J. Hahn, B. Ridley, J. Walega, J. Greenberg, L. Heidt, and P. Zimmerman (1992), Alkyl nitrates and selected halocarbon measurements at Mauna-Loa observatory, Hawaii, *J. Geophys. Res.*, *97*(D10), 10,331–10,348.

Bernsten, T. J., S. Karlsdottir, and D. A. Jaffe (1999), Influence of Asian emissions on the composition of air reaching the north western United States, *Geophys. Res. Lett.*, *26*(14), 2171–2174.

Brock, C. A., et al. (2004), Particle characteristics following cloud-modified transport from Asia to North America, *J. Geophys. Res.*, *109*, D23S26, doi:10.1029/2003JD004198, in press.

Carmichael, G. R., D. G. Streets, G. Calori, M. Amann, M. Z. Jacobson, J. Hansen, and H. Ueda (2002), Changing trends in sulfur emissions in Asia: Implications for acid deposition, air pollution, and climate, *Environ. Sci. Technol.*, *36*, 4707–4713.

Clemitshaw, K. C., J. Williams, O. V. Rattigan, D. E. Shallcross, K. S. Law, and R. A. Cox (1997), Gas-phase ultraviolet absorption cross-sections and atmospheric lifetimes of several C_2–C_5 alkyl nitrates, *J. Photochem. Photobiol. A*, *102*, 117–126.

Cooper, O. R., et al. (2004a), A case study of transpacific warm conveyor belt transport: Influence of merging airstreams on trace gas import to North America, *J. Geophys. Res.*, *109*, D23S08, doi:10.1029/2003JD003624.

Cooper, O. R., et al. (2004b), On the life cycle of a stratospheric intrusion and its dispersion into polluted warm conveyor belts, *J. Geophys. Res.*, *109*, D23S09, doi:10.1029/2003JD004006.

de Gouw, J. A., C. Warneke, T. Karl, G. Eerdekens, C. van der Veen, and R. Fall (2003a), Sensitivity and specificity of atmospheric trace gas detection by proton-transfer reaction mass spectrometry, *Int. J. Mass Spectrom. Ion Processes*, *223*(1–3), 365–382.

de Gouw, J. A., C. Warneke, D. D. Parrish, J. S. Holloway, M. Trainer, and F. C. Fehsenfeld (2003b), Emission sources and ocean uptake of acetonitrile (CH_3CN) in the atmosphere, *J. Geophys. Res.*, *108*(D11), 4329, doi:10.1029/2002JD002897.

de Gouw, J. A., P. D. Goldan, C. Warneke, W. C. Kuster, J. M. Roberts, M. Marchewka, S. B. Bertman, A. A. P. Pszenny, and W. C. Keene (2003c), Validation of proton transfer reaction-mass spectrometry (PTR-MS) measurements of gas-phase organic compounds in the atmosphere during the New England Air Quality Study (NEAQS) in 2002, *J. Geophys. Res.*, *108*(D21), 4682, doi:10.1029/2003JD003863.

de Gouw, J. A., et al. (2004), Chemical composition of air masses transported from Asia to the U.S. West Coast during ITCT 2K2: Fossil fuel combustion versus biomass-burning signatures, *J. Geophys. Res.*, *109*, D23S20, doi:10.1029/2003JD004202, in press.

Eisele, F. L., and D. J. Tanner (1993), Measurement of the gas phase concentration of H_2SO_4 and methane sulfonic acid and estimates of H_2SO_4 production and loss in the atmosphere, *J. Geophys. Res.*, *98*(D5), 9001–9010.

Fiore, A. M., D. J. Jacob, I. Bey, R. M. Yantosca, B. D. Field, A. C. Fusco, and J. G. Wilkinson (2002), Background ozone over the United States in summer: Origin, trend, and contribution to pollution episodes, *J. Geophys. Res.*, *107*(D15), 4275, doi:10.1029/2001JD000982.

Fischer, H., F. G. Wienhold, P. Hoor, O. Bujok, C. Schiller, P. Siegmund, M. Ambaum, H. A. Scheeren, and J. Lelieveld (2000), Tracer correlations in the northern high latitude lowermost stratosphere: Influence of cross-tropopause mass exchange, *Geophys. Res. Lett.*, *27*(1), 97–100.

Flocke, F. A., A. Volz-Thomas, and D. Kley (1991), Measurements of alkyl nitrates in rural and pollutes air masses, *Atmos. Environ., Part A*, *25*, 1951–1960.

Forster, C., et al. (2004), Lagrangian transport model forecasts and a transport climatology for the Intercontinental Transport and Chemical Transformation 2002 (ITCT 2K2) measurement campaign, *J. Geophys. Res.*, *109*, D07S92, doi:10.1029/2003JD003589.

Heidt, L. E., J. F. Vedder, W. H. Pollock, R. A. Lueb, and B. E. Henry (1989), Trace gases in the Antarctic atmosphere, *J. Geophys. Res*, *94*(D9), 11,599–11,611.

Heikes, B. G., et al. (2002), Atmospheric methanol budget and ocean implication, *Global Biogeochem. Cycles*, *16*(4), 1133, doi:10.1029/2002GB001895.

Hess, P. G., and T. Vukicevic (2003), Intercontinental transport, chemical transformations, and baroclinic systems, *J. Geophys. Res.*, *108*(D12), 4354, doi:10.1029/2002JD002798.

Hoell, J. M., D. D. Davis, S. C. Liu, R. Newell, M. Shipham, H. Akimoto, R. J. McNeal, R. J. Bendura, and J. W. Drewry (1996), Pacific Exploratory Mission-West A (PEM West A): September–October 1991, *J. Geophys. Res.*, *101*(D1), 1641–1653.

Hoell, J. M., D. D. Davis, S. C. Liu, R. E. Newell, H. Akimoto, R. J. McNeal, and R. J. Bendura (1997), The Pacific Exploratory Mission-West Phase B: February–March, 1994, *J. Geophys. Res.*, *102*(D23), 28,223–28,240.

Holloway, J. S., R. O. Jakoubak, D. D. Parrish, C. Gerbig, A. Volz-Thomas, S. Schmitgen, A. Fried, B. Wert, B. Henry, and J. R. Drummond (2000), Airborne intercomparison of vacuum ultraviolet fluorescence and tunable diode laser absorption measurements of tropospheric carbon monoxide, *J. Geophys. Res.*, *105*(D19), 24,251–24,261.

Huebert, B. J., T. Bates, P. B. Russell, G. Shi, Y. J. Kim, K. Kawamura, G. Carmichael, and T. Nakajima (2003), An overview of ACE-Asia: Strategies for quantifying the relationships between Asian aerosols and their climatic impacts, *J. Geophys. Res.*, *108*(D23), 8633, doi:10.1029/2003JD003550.

Jacob, D. J., J. A. Logan, and P. P. Murti (1999), Effect of rising Asian emissions on surface ozone in the U.S., *Geophys. Res. Lett.*, *26*(D14), 2175–2178.

Jacob, D. J., B. D. Field, E. M. Jin, I. Bey, Q. Li, J. A. Logan, R. M. Yantosca, and H. B. Singh (2002), Atmospheric budget of acetone, *J. Geophys. Res.*, *107*(D10), 4100, doi:10.1029/2001JD000694.

Jacob, D. J., J. H. Crawford, M. M. Kleb, V. S. Connors, R. J. Bendura, J. L. Raper, G. W. Sachse, J. C. Gille, L. Emmons, and C. L. Heald (2003), Transport and Chemical Evolution Over the Pacific (TRACE-P) aircraft mission: Design, execution, and first results, *J. Geophys. Res.*, *108*(D20), 9000, doi:10.1029/2002JD003276.

Jaffe, D. A., et al. (1999), Transport of Asian air pollution to North America, *Geophys. Res. Lett.*, *26*(6), 711–714.

Jaffe, D. A., T. Anderson, D. Covert, B. Trost, J. Danielson, W. Simpson, D. Blake, J. Harris, and D. Streets (2001), Observations of ozone and related species in the northeast Pacific during the PHOBEA campaigns: 1. Ground based observations at Cheeka Peak, *J. Geophys. Res.*, *106*(D7), 7449–7461.

Jaffe, D., H. Price, D. Parrish, A. Goldstein, and J. Harris (2003a), Increasing background ozone during spring on the west coast of North America, *Geophys. Res. Lett.*, *30*(12), 1613, doi:10.1029/2003GL017024.

Jaffe, D., I. McKendry, T. Anderson, and H. Price (2003b), Six 'new' episodes of trans-Pacific transport of air pollutants, *Atmos. Environ.*, *37*, 391–404.

Kato, N., and H. Akimoto (1992), Anthropogenic emissions of SO_2 and NO_x in Asia: Emission inventories, *Atmos. Environ., Part A*, *26*, 2997–3017.

Koike, M., et al. (2003), Export of anthropogenic reactive nitrogen and sulfur compounds from the east Asia region in spring, *J. Geophys. Res.*, *108*(D20), 8789, doi:10.1029/2002JD003284.

Kotchenruther, R. A., D. A. Jaffe, H. J. Beine, T. L. Anderson, J. W. Bottenheim, J. M. Harris, D. R. Blake, and R. Schmitt (2001a), Observations of ozone and related species in the northeast Pacific during the PHOBEA campaigns: 2. Airborne observations, *J. Geophys. Res.*, *106*(D7), 7463–7483.

Kotchenruther, R. A., D. A. Jaffe, and L. Jaegle (2001b), Ozone photochemistry and the role of peroxyacetyl nitrate in the springtime northeastern Pacific troposphere: Results from the Photochemical Ozone Budget of the Eastern North Pacific Atmosphere (PHOBEA) campaign, *J. Geophys. Res.*, *106*(D22), 28,731–28,741.

Miyazaki, Y., et al. (2003), Synoptic-scale transport of reactive nitrogen over the western Pacific in spring, *J. Geophys. Res.*, *108*(D20), 8788, doi:10.1029/2002JD003248.

Moore, K. G., II, A. D. Clarke, V. N. Kapustin, and S. G. Howell (2003), Long-range transport of continental plumes over the Pacific Basin: Aerosol physiochemistry and optical properties during PEM-Tropics A and B, *J. Geophys. Res.*, *108*(D2), 8236, doi:10.1029/2001JD001451.

Moxim, W. J., H. Levy, and P. S. Kasibhatla (1996), Simulated global tropospheric PAN: Its transport and impact on NOx, *J. Geophys. Res.*, *101*(D7), 12,621–12,638.

Neuman, J. A., et al. (2002), Fast-response airborne in situ measurements of HNO_3 during the Texas 2000 Air Quality Study, *J. Geophys. Res.*, *107*(D20), 4436, doi:10.1029/2001JD001437.

Neuman, J. A., et al. (2003), Variability in ammonium nitrate formation and nitric acid depletion with altitude and location over California, *J. Geophys. Res.*, *108*(D17), 4557, doi:10.1029/2003JD003616.

Nicks, D. K., et al. (2003), Fossil-fueled power plants as a source of atmospheric carbon monoxide, *J. Environ. Monit.*, *5*(1), 35–39.

Novelli, P. C., K. A. Masarie, and P. M. Lang (1998), Distributions and recent changes of carbon monoxide in the lower troposphere, *J. Geophys. Res.*, *103*(D15), 19,015–19,033.

Parrish, D. D., C. J. Hahn, E. J. Williams, R. B. Norton, and F. C. Fehsenfeld (1992), Indications of photochemical histories of Pacific air masses from measurements of atmospheric trace species at Point Arena, California, *J. Geophys. Res.*, *97*(D14), 15,883–15,901.

Parrish, D. D., M. Trainer, J. S. Holloway, J. E. Yee, M. S. Warshawsky, and F. C. Fehsenfeld (1998), Relationships between ozone and carbon monoxide at surface sites in the North Atlantic region, *J. Geophys. Res.*, *103*(D11), 13,357–13,376.

Price, H., D. Jaffe, P. V. Doskey, I. McKendry, and T. Anderson (2003), Vertical profiles of O_3, aerosols, CO, and NMHCs in the northeast Pacific during the TRACE-P and ACE-Asia experiments, *J. Geophys. Res.*, *108*(D20), 8799, doi:10.1029/2002JD002930.

Ridley, B. A., F. E. Grahek, and J. G. Walega (1992), A small, high-sensitivity, medium response ozone detector suitable for measurements from light aircraft, *J. Atmos. Oceanic Technol.*, *9*(2), 142–148.

Ridley, B. A., E. L. Atlas, J. G. Walega, G. L. Kok, T. A. Staffelbach, J. P. Greenberg, F. E. Grahek, P. G. Hess, and D. D. Montzka (1997), Aircraft measurements made during the spring maximum of ozone over Hawaii: Peroxides, CO, O_3, NOy, condensation nuclei, selected hydrocarbons, halocarbons, and alkyl nitrates between 0.5 and 9 km altitude, *J. Geophys. Res.*, *102*(D15), 18,935–18,961.

Roberts, J. M. (1990), The atmospheric chemistry of organic nitrates, *Atmos. Environ., Part A*, *24*, 243–287.

Roberts, J. M., and R. W. Fajer (1989), UV absorption cross-sections of organic nitrates of potential atmospheric importance and estimation of atmospheric lifetimes, *Environ. Sci. Technol.*, *23*, 945–951.

Roberts, J. M., et al. (1998), Measurements of PAN, PPN, and MPAN made during the 1994 and 1995 Nashville Intensives of the Southern Oxidant Study: Implications for regional ozone production from biogenic hydrocarbons, *J. Geophys. Res.*, *103*(D17), 2473–2490.

Ryerson, T. B., et al. (1998), Emissions lifetime and ozone formation in power plant plumes, *J. Geophys. Res.*, *103*(D17), 22,569–22,583.

Ryerson, T. B., L. G. Huey, K. Knapp, J. A. Neuman, D. D. Parrish, D. T. Sueper, and F. C. Fehsenfeld (1999), Design and initial characterization of an inlet for gas-phase NOy measurements, *J. Geophys. Res.*, *104*(D5), 5483–5492.

Ryerson, T. B., E. J. Williams, and F. C. Fehsenfeld (2000), An efficient photolysis system for fast-response NO_2 measurements, *J. Geophys. Res.*, *105*(D21), 26,447–26,461.

Schauffler, S., E. L. Atlas, D. R. Blake, F. Flocke, R. A. Lueb, M. Lee-Taylor, V. Stroud, and W. Travicek (1999), Distributions of brominated organic compounds in the troposphere and lower stratosphere, *J. Geophys. Res.*, *104*(D17), 21,513–21,535.

Singh, H. B., L. J. Salas, and W. Viezee (1986), Global distribution of peroxyacteyl nitrate, *Nature*, *321*(6070), 588–591.

Stohl, A., M. Trainer, T. B. Ryerson, J. S. Holloway, and D. D. Parrish (2002), Export of NOy from the North American boundary layer during 1996 and 1997 North Atlantic Regional Experiments, *J. Geophys. Res.*, *107*(D11), 4131, doi:10.1029/2001JD000519.

Streets, D. G., and S. T. Waldhoff (2000), Present and future emissions of air pollutants in China: SO_2, NOx, and CO, *Atmos. Environ.*, *34*, 364–374.

Streets, D., et al. (2003), An inventory of gaseous and primary aerosol emissions in Asia in the year 2000, *J. Geophys. Res.*, *108*(D21), 8809, doi:10.1029/2002JD003093.

Takegawa, N., et al. (2003), Removal of NOx and NOy in biomass burning plumes in the boundary layer over northern Australia, *J. Geophys. Res.*, *108*(D10), 4308, doi:10.1029/2002JD002505.

Talbot, R. W., et al. (1997), Large-scale distributions of tropospheric nitric, formic, and acetic acids over the western Pacific Basin during wintertime, *J. Geophys. Res.*, *102*(D23), 28,303–28,313.

Talukdar, R. K., J. B. Burkholder, A. M. Schmoltner, J. M. Roberts, R. R. Wilson, and A. R. Ravishankara (1995), Investigation of the loss processes for peroxyacetyl nitrate in the atmosphere: UV photolysis and reaction with OH, *J. Geophys. Res.*, *100*(D17), 14,163–14,173.

Talukdar, R. K., J. B. Burkholder, M. Hunter, M. K. Gilles, J. M. Roberts, and A. R. Ravishankara (1997), Atmospheric fate of several alkyl nitrates: Part 2. UV absorption cross-sections and photodissociation quantum yields, *J. Chem. Soc. Faraday Trans.*, *93*, 2797–2805.

van Aardenne, J. A., G. A. Carmichael, H. Levy, D. Streets, and L. Hordijk (1999), Anthropogenic NOx emissions in Asia in the period 1990–2020, *Atmos. Environ.*, *33*, 633–646.

Wallace, J. M., and P. V. Hobbs (1977), *Atmospheric Science: An Introductory Survey*, 467 pp., Academic, San Diego, Calif.

Warneke, C., D. A. De Gouw, W. C. Kuster, P. D. Goldan, and R. Fall (2003), Validation of atmospheric VOC measurements by proton-transfer-reaction mass spectrometry using a gas-chromatographic pre-separation method, *Environ. Sci. Technol.*, *37*, 2494–2501, doi:10.1021/es026266i.

E. Atlas, RSMAS/MAC, University of Miami, Miami, FL 33149, USA. (eatlas@rsmas.miami.edu)

O. R. Cooper, J. A. de Gouw, E. Dunlea, F. C. Fehsenfeld, J. S. Holloway, G. Hübler, J. A. Neuman, J. B. Nowak, D. D. Parrish, J. M. Roberts, T. B. Ryerson, and C. Warneke, Aeronomy Laboratory, National Oceanic and Atmospheric Administration, R/AL-7, 325 Broadway, Boulder, CO 80305, USA. (cooper@al.noaa.gov; jdegouw@al.noaa.gov; edunlea@al.noaa.gov; fcf@al.noaa.gov; jholloway@al.noaa.gov; ghubler@al.noaa.gov; neuman@al.noaa.gov; jnowak@al.noaa.gov; dparrish@al.noaa.gov; jr@al.noaa.gov; tryerson@al.noaa.gov; cwarneke@al.noaa.gov)

S. Donnelly, Department of Chemistry, Fort Hays State University, Hays, KS 67601, USA.

F. Flocke and S. Schauffler, Atmospheric Chemistry Division, National Center for Atmospheric Research, P. O. Box 3000, Boulder, CO 80305, USA. (ffl@acd.ucar.edu; sues@acd.ucar.edu)

L. G. Huey and D. J. Tanner, School of Earth and Atmospheric Sciences, Georgia Institute of Technology, 221 Bobby Dodd Way, Atlanta, GA 30332, USA. (greg.huey@eas.gatech.edu; david.tanner@eas.gatech.edu)

D. K. Nicks Jr., Ball Aerospace and Technologies Corporation, P. O. Box 1062, Boulder, CO 80301, USA.